Case Studies in Thermal Engineering 45 (2023) 103010

Contents lists available at ScienceDirect

Case Studies in Thermal Engineering

journal homepage: www.elsevier.com/locate/csite

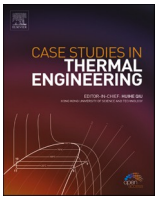

Performance degradation of air source heat pumps under faulty conditions

Alfonso William Mauro *, Francesco Pelella, Luca Viscito

Department of Industrial Engineering, Università degli Studi di Napoli – Federico II, P.le Tecchio 80, 80125, Naples, Italy

ARTICLE INFO

Handling Editor: Huihe Qiu

Keywords:
Heat pumps
Physics-based model
Soft faults
Seasonal performance degradation
Fault detection
Diagnosis and evaluation

ABSTRACT

The ongoing European regulations towards the decarbonization of energy intensive sectors such as heating and cooling will lead to an increase of heat pump appliances. Apart from anomalies that can be detected in a preliminary phase after the start-up, soft faults such as refrigerant leakage and heat exchanger fouling may cause a performance degradation in such systems that evolves in time and that must be detected before it becomes too big. From this perspective, in a previous paper (Pelella et al. [1]) it has been demonstrated that, in cooling mode, a seasonal performance penalization up to 50% can be reached in case of a not-planned maintenance scenario, whereas wherever a timed or intelligent maintenance strategy is implemented based on data-monitoring, this impact can be significantly reduced. Therefore, in order to extend the analysis previously carried out to the heating cases, and to evaluate the consequent energetic degradation of the system in case of soft faults occurring, depending on different climate conditions and maintenance scenarios, this paper develops a physic-based model to simulate system components and to describe the fault phenomenology on a residential 2.6 kW air-to-air heat pump, operating in winter mode. The results show that in heating mode a 40% condenser fouling and a 30% refrigerant leakage cause a performance degradation of respectively 16% and 12%, whereas in case of evaporator fouling the performance penalization is only of 3.2%. Moreover, the performance degradation is enhanced by the overlapping effect of simultaneous faults. Finally, from seasonal simulations of the heat pump along an entire machine lifetime of 12 years, it is found that none of the maintenance strategies analysed is able to significantly reduce the number of scenarios penalized by faults, opening to the potential development of systems for the automatic fault detection, diagnosis, and evaluation (FDDE).

Nomenclature

Roman

COP	Coefficient of performance [−]
$COP_{penaliz}$	COP degradation [%]
Dis	Compressor displacement [m^3]
f_{ee}	Conversion factor for electricity production [$kgCO_2/kWh$]
$FI_{co,ev,leak}$	Fault Intensity for condenser fouling, evaporator fouling and refrigerant leakage [%]
GWP	Global Warming Potential [kg_{co2}/kg_{ref}]

* Corresponding author.
E-mail address: wmauro@unina.it (A.W. Mauro).

https://doi.org/10.1016/j.csite.2023.103010
Received 17 December 2022; Received in revised form 31 March 2023; Accepted 12 April 2023
Available online 12 April 2023

h	Specific Enthalpy [kJ/kg]
K_1, K_2	Valve mass flow rate calibration coefficient [−]
m	Refrigerant charge [kg]
$\dot{m}$	Mass flow rate [kg/s]
n	Compressor rotation speed [−]
p	Pressure [bar]
Q	Thermal Energy [kWh]
$\dot{Q}$	Thermal Power [kW]
R	Thermal Resistance [K/W]
s	Specific Entropy [kJ/kgK]
S	Transverse Cross-Section [m^2]
S_{ht}	Heat transfer surface [m^2]
SCOP	Seasonal coefficient of performance [−]
T	Temperature [°C]
TEWI	Total Equivalent Warming Impact [$kgCO_2$]
UA	Thermal Conductance [W/K]
v	Specific volume [m^3/kg]
$\dot{V}$	Volumetric flow rate [m^3/s]
W	Electric Energy [kWh]
$\dot{W}$	Electric Power [kW]
x	Vapor quality [−]
z	Position along the tube [m]

Greek

α	Void Fraction [−]
Δ	Variation [−]
η	Efficiency [−]
ξ	Valve percentage opening [−]
ρ	Density [kg/m^3]

Subscripts

air	Related to air
amb	Ambient
c	Convective
co	Condenser
comp	Compressor
el	Electric
ev	Evaporator
ext	External
fan	Related to fans
foul	Fouling fault
free-flow	Free-flow sectional area
g	Global
id	Ideal
in	Related to the inlet
int	Internal
is	Isentropic
k	Conductive
L	Liquid Phase
leak	Leaked
max	Maximum
out	Related to the outlet
ref	Related to refrigerant
sp	Single phase
sh	Superheating
tot	Total
tp	Two-phases
v	Volumetric
V	Vapor Phase

1. Introduction

Nowadays, the building sector contributes for almost 20% of the global energy consumption [2], whereas heating and cooling represent approximately the 75% of the final energy consumption in residential buildings [3]. These energy intensive sectors have to be decarbonized to achieve all the fixed goals of the COP26 conference [4] to limit the ambient temperature increase to +1.5 °C [5] compared with the pre-industrial era. Therefore, for heating and cooling sectors, the achievement of these targets can only be obtained with the spreading of heat pumps, that well fit in future scenarios where the renewable energy share will increase.

In order to further reduce the direct and indirect environmental impacts of these systems, several future opportunities are being adopted. New refrigerants are being studied among blends [6–8] and natural fluids [9], to reduce the direct emissions related to refrigerant leakage deriving mainly from pipe or joint failures and leaking seal/gland/core of the compressor pack and in high-pressure lines [10]. Regarding the indirect contributions, instead, the presence of anomalies can reduce system performances. It is the case of the so-called soft faults, such as heat exchanger fouling, refrigerant leakage, etc., which do not compromise the continuous operation of machines, and for that reason they can remain unidentified for long periods of time, causing a degradation in performance [11].

Hence, self-fault detection, diagnosis and evaluation (FDDE) tools are being developed in order to limit the effect of faults on system performance. Most of them take advantage of artificial intelligence and machine learning which are spreading in recent years in refrigeration and heat pumps field [12] with several purposes of fault detection and diagnosis [13], energy performance prediction [14], optimization and control [15].

Therefore, in order to identify the most influenced parameters by faults, several experimental works and numerical investigations have been carried out. A 316 kW Centrifugal chiller has been investigated by Comstock and Braun [16], which analyse the influence of condenser and evaporator improper secondary fluid flows and fouling, improper refrigerant charge, presence of non-condensable in the refrigerant and others on 64 different measured variables of an experimental apparatus. Rooftop units have been studied experimentally by Breuker and Braun [17] for refrigerant leakage and numerically by Kim et al. [18] for the soft faults of condenser fouling, liquid line restriction, presence of non-condensable, refrigerant leakage and overcharge. Water heat pumps instead have been studied by Grace et al. [19], which analysed the effect of the refrigerant charge amount on a 4 kW R404A water chiller, and by Bellanco et al. [20], which studied evaporator fouling, refrigerant overcharge, compressor valve leakage and liquid line restriction on a 10 kW propane water heat pump. Split systems have been treated for fin-and-tube heat exchanger fouling by Qureshi and Zubair [21] and by Mehrabi and Yuill [22], whereas other soft faults related to improper secondary flow, liquid line restriction, improper refrigerant charge and non-condensable in the refrigerant have been studied by Hu et al. [23]. Finally, Mehrabi and Yuill [24,25] analysed the effect of several soft faults on different typology of systems, trying to give a generalization of the connections between faults and symptoms for all the kinds of systems investigated.

Among the works analysed by the literature, only a few of them dealt with small capacity system for residential heating and cooling, and only the works of Hu et al. [26] for split systems and Zhou et al. [27] for variable refrigerant volume (VRVs) systems analysed the effect on the thermodynamic cycle of simultaneous occurring faults. All these aspects were deepened in Pelella et al. [1] in which we analysed the effect of standalone and simultaneous occurring refrigerant leakage, condenser and evaporator fouling for an air-to-air heat pump operating in cooling mode. In the aforementioned paper, the effect of faults on performance is quantified both on the coefficient of performance (COP) value in nominal steady-state conditions, and on the seasonal coefficient of performance (SCOP) along the entire machine lifetime. Considering not-planned maintenance strategies, SCOP penalizations over 50% are reached, caused by the uncontrolled fault evolutions along the 12 years machine lifetime. The penalization are significantly reduced by adopting time-based maintenance strategies (every 4, 2 and 1 year), and with intelligent FDDE strategies able to lead to a maintenance intervention only if the COP penalization becomes significant, without any extra-maintenance costs.

However, our previous work has filled several gaps and demonstrated several aspects only related to the cooling mode, and only for some cooling predominant climatic conditions. Therefore, the main target of this paper is to carry out the same investigation, but for the heating mode, to understand if remarks are replicable also for this operating mode and considering heating predominant climate conditions.

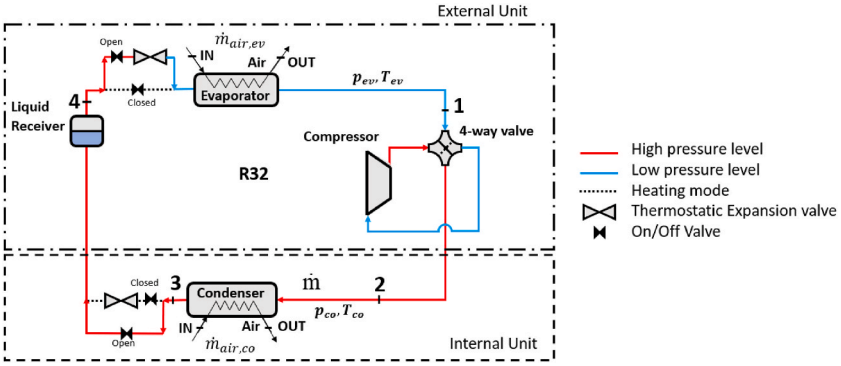

Fig. 1. Schematic of the air-to-air heat pump modelled in this work, operating in heating mode.

2. Components models

The system modelled is a reversible air-to-air heat pump for domestic heating and cooling. The machine is composed of two units, one external and one internal. The external unit is composed of a scroll compressor, a 4-way valve able to switch between heating and cooling modes, a fin-and-tube heat exchanger used as an evaporator in heating mode (condenser in cooling mode), a thermostatic expansion valve for the heating mode, able to control evaporator superheating, and a liquid receiver. The internal unit instead is composed of a fin-and-tube heat exchanger employed as a condenser in heating mode (evaporator in cooling mode) and a thermostatic expansion valve for the cooling mode. In Fig. 1 a schematic of the machine operating in heating mode is provided. Both fin-and-tube heat exchangers have been considered with plain fins. Other components such as 2 and 4-way valves are employed in order to guarantee a correct reversion of the thermodynamic cycle between operating modes. The working fluid for the system investigated is R32, which is commonly used for such small capacity air conditioning systems.

Sub-models for each of the components of the system analysed are then developed, as already done in our previous works [28–30]. Regarding fin-and-tube heat exchangers, they have been divided into several infinitesimal volumes, and for each of them the global conductance is evaluated considering internal and external convective thermal resistances, and the conduction through the metal, as follow:

$$dUA = \frac{1}{dR_{c,int} + dR_k + dR_{c,ext}} \tag{1}$$

The first row of the heat exchanger is then integrated evaluating refrigerant and air temperatures and, once completed, another row is added until all the heat exchanger rows are calculated. For the evaluation of each of the thermal resistances, both aspects related to geometry and heat transfer characterization have been considered in the model. The geometric characterization aims to evaluate the effective internal and external heat transfer surfaces, the number of tubes, of rows and tubes per row, and others, and it has been carried out according to Shah and Sekulic [31]. Effective air mass flow rates are evaluated through the coupling between heat exchanger fans and coils, considering typical characteristic curves of a tangential blower for the internal unit and an axial fan for the external unit. Regarding the heat transfer characterization, conductive heat transfer coefficients have been evaluated through well-known empirical correlations from the literature. For instance, for flow boiling and flow condensation, correlations of respectively Gungor and Winterton [32] and Shah [33] have been employed, whereas the superheated vapor heat transfer coefficient has been calculated with the correlation of Dittus and Boelter [34]. Regarding air instead, heat transfer coefficient and pressure drops are evaluated with the Wang [35] correlations for plain fins, whereas the fin efficiency is calculated using the Schmidt [36] approximation.

Regarding the thermostatic expansion valve, the following expression to evaluate the valve mass flow rate depending on the pressure drop across the valve has been used.

$$\dot{m}_{valve} = \xi \bullet \rho_{in} \bullet K_1 \bullet \sqrt{\frac{2 \bullet \overline{v}_{in-out,is} \bullet (p_{in} - p_{out})}{\left(\frac{\rho_{in}^2}{\rho_{out,is}^2} \bullet K_2 - 1\right)}} \tag{2}$$

$\overline{v}_{in-out,is}$ is the average specific volume along the isentropic, whereas $p_{in/\ out}$ and $\rho_{in/out}$ are pressures and densities at the inlet and the outlet. ξ is the valve opening percentage, whereas K_1 and K_2 are calibration coefficients fitted on manufacturer data.

The presence of a liquid receiver causes that the thermostatic expansion valve is always fed with saturated liquid (x = 0), if the refrigerant charge amount is enough to avoid that the liquid receiver becomes empty. The refrigerant charge amount requested by the user depending on external boundary conditions has been evaluated considering the contributions of the two internal and external heat exchangers, and of the liquid line after the condenser, neglecting the refrigerant charge in the suction and discharge lines of the compressor. Therefore, the total amount is considered as the sum of the one-phase and two-phase contributions, evaluated for an infinitesimal control volume as follows:

$$m_{tot} = m_{sp} + m_{tp} \tag{3}$$

$$dm_{sp} = \rho\, S dz \tag{4}$$

$$dm_{tp} = S[\rho_L(1-\alpha) + \rho_V \alpha] dz \tag{5}$$

For the two-phase contribution, the volumetric void fraction α has been evaluated with the Rouhani and Axelsson [37] correlation.

Regarding the scroll compressor, the following expression is used to evaluate respectively the mass flow rate:

$$\dot{m}_{comp} = \rho_{in} \bullet \eta_v \bullet \frac{n}{60} \bullet Dis \tag{6}$$

ρ_{in} is the inlet compressor density, n is the rotational speed, whereas *Dis* and η_v are respectively the compressor displacement and the volumetric efficiency. Both of them have been calibrated on manufacturer data.

Finally, once able to evaluate all the states of the thermodynamic cycles, thermal power to the condenser, electrical powers for the compressor and heat exchanger fans, and COP are evaluated through energy balances, as follows:

$$\dot{Q}_{co} = \dot{m}_{comp} \bullet \left(h_{in,co} - h_{out,co}\right) \tag{7}$$

$$\dot{W}_{fan} = \frac{\Delta p_{air} \bullet \dot{V}_{air}}{\eta_{fan}} \rightarrow \eta_{fan} = 0.65 \tag{8}$$

$$\dot{W}_{comp} = \dot{m}_{comp} \bullet \frac{\left(h_{out,is,comp} - h_{in,comp}\right)}{\eta_g} \tag{9}$$

$$COP = \frac{\dot{Q}_{co}}{\left(\dot{W}_{comp} + \dot{W}_{fan}\right)} \tag{10}$$

η_g is the compressor global efficiency, also calibrated on manufacturer data. Further details about the calibration processes for the compressor and the valve, and about the resolution algorithm employed to simulate the behaviour of the entire system, are provided in previous works [1,38].

3. Faults modelling

Among all the common soft faults for heat pumps, it has been decided to study refrigerant leakage, condenser fouling and evaporator fouling. As a matter of fact, as also clarified in Pelella et al. [38], these three faults have been chosen because other kinds of soft anomalies are usually related to improper installation or maintenance operations and therefore can be identified in a small time after the start-up (such as non-condensable in the refrigerant, defective expansion valve), or are related to single components (such compressor ageing, valve leakage, defective expansion valve), and so they can be identified with dedicated models on the component itself.

Regarding heat exchanger fouling, different methodologies have been adopted for respectively external and internal units. In Fig. 2 is shown an elementary geometry of a fin-and-tube heat exchanger, in case of clean surfaces (Fig. 2(a)) and in case of fouling of the internal (Fig. 2(b)) and external (Fig. 2(c)) units.

Regarding the internal unit fouling, a filter is usually installed on the condenser to prevent the infiltration of dust particles on the fin and tube surfaces [39]. The fouling evolution manifests itself as an accumulation of dust on the filter, causing an air mass flow rate reduction (Fig. 2(b)). Therefore, to simulate this kind of fault, a fault intensity factor equal to the air mass flow rate penalization compared with the clean heat exchanger has been defined as follows.

$$FI_{foul,ev} = \frac{\dot{V}_{free-flow,foul}}{\dot{V}_{free-flow,clean}} \bullet 100 \tag{11}$$

This approach is in accordance with the one of Breuker and Braun [17], who artificially simulated the internal unit fouling by reducing the mass flow rate of the secondary fluid. Therefore, once assigned an evaporator fouling fault intensity, the air mass flow rate can be evaluated by Eq. (11), whereas the heat transfer surface remains unchanged with respect to the fault-free condition case.

Regarding the external unit instead, according to several experimental evidences [40,41], a preliminary fouling tends to accumulate on the face-front of the heat exchanger, causing an enhancement of the heat transfer in the initial period. On the other hand, a high fouling accumulation level can cause that several portions of the heat exchangers are completely blocked, with a local velocity close to zero, as shown in Fig. 2(c). This results to be a dual penalization, both on the free-flow area of air across the heat exchanger coil, and on the heat transfer surface of the heat exchanger. Therefore, in order to simulate the effect of the external unit fouling, used as evaporator in winter mode, the following definition of the fault intensity for this fault is adopted:

$$FI_{foul,co} = \frac{S_{free-flow,foul}}{S_{free-flow,clean}} \bullet 100 = \frac{S_{ht,foul}}{S_{ht,clean}} \bullet 100 \tag{12}$$

The free-flow penalization evaluated through Eq. (12) causes an increase of pressure drops across the heat exchanger coil, and consequently the new reduced air mass flow rate is evaluated from the new coupling point between fans and heat exchangers. The new

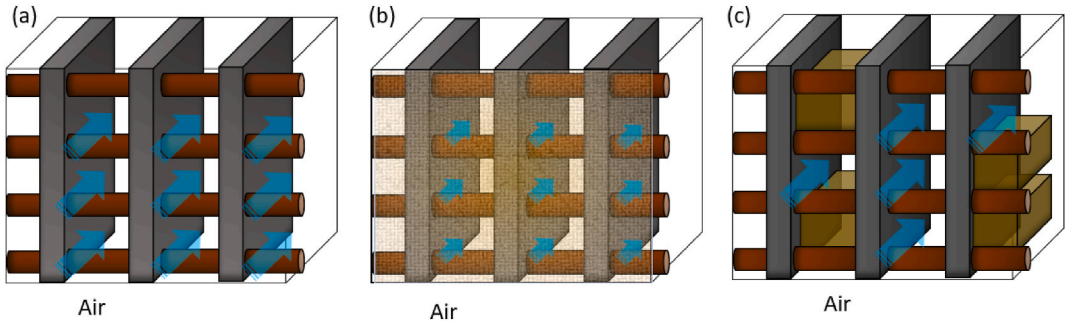

Fig. 2. Elementary geometry for a fin-and-tube heat exchangers. (a) Clean surfaces; (b) Fouling of the internal unit (condenser in heating mode) with dust accumulated on the face-front filter; (c) Fouling of the external unit (evaporator in heating mode) with portions blocked by dust.

heat transfer surface penalization instead can be directly evaluated through Eq. (12). This kind of approach is able to simulate both particulate and freezing fouling, which are the two predominant fouling mechanisms in the winter season [42]. Moreover, this methodology is in accordance with the one employed by Breuker and Braun [17], which uses vertical cardboard strip on the face-front of the heat exchanger, in order to experimentally simulate the presence of this kind of fault.

For refrigerant leakage modelling, the definition of fault intensity for such fault has been considered as the percentage difference between the actual refrigerant charge of the system and the nominal value, according to Mehrabi and Yuill [24]. The latter has been assumed as the maximum value requested by the system in all the boundary conditions investigated in winter mode.

$$FI_{leak} = \frac{m_{nominal} - m_{actual}}{m_{nominal}} \bullet 100 \tag{13}$$

When a refrigerant leakage occurs in the model, we imposed a faulty condition whenever the liquid receiver becomes empty. The effective refrigerant charge amount requested is evaluated through equations (3) and (4) depending on the external boundary conditions. Assumed a saturated liquid at the exit of the liquid receiver, when the fault intensity is fixed to a value such that the required amount of charge for the actual boundary conditions is less than the one currently available in the system, the extra amount of refrigerant is stored in the accumulator. If instead the required amount, under the assumption of saturated liquid at the exit of the liquid receiver, is higher than the one actually available, the model starts assuming an increasing vapor quality at the exit of the liquid receiver up to the amount required is equal to the one actually available. The thermostatic valve started to be fed with a saturated vapor, with a certain vapor quality ($x_{in,valve}$), resulting in a valve chocking and in a mass flow rate decrease. Consequently, this reduction causes a variation in the coupling point between the compressor and the valve, and therefore a reduction also of the evaporating temperature, as shown in Fig. 3. In the end, all these aspects cause a penalization both in thermal powers and in the system performance.

Consistently to the description made, the fault intensity for the refrigerant charge corresponding to the moment when the liquid receiver becomes empty depends on the initial amount of refrigerant charge. The assumption behind is to have an empty liquid receiver when the boundary conditions requires the maximum refrigerant charge (maximum evaporation temperature equal to 12 °C and maximum condensation temperature equal to 40 °C), which is the minimum refrigerant charge required to have a proper working of the system under extreme conditions without a refrigerant loss.

4. Case study data and model calibration

The analysed case study is a rated 2.6 kW air-to-air residential heat pump for domestic heating. The system is the same studied in the work of Pelella et al. [1], but inverting the two heat exchangers. The working fluid employed is R32, and the thermostatic expansion valve controls a target superheating of 7 °C. The rated refrigerant charge of the system is 490 g. Other rated parameters of the system and geometrical characteristics of the heat exchangers are provided in Table 1. It is worth noting that all the components (compressor, heat exchangers) have been designed to operate properly in cooling mode, with the internal evaporator unit able to provide a thermal power of 2.60 kW, and an external condenser unit a thermal power of 3.31 kW, for fixed ambient/indoor temperatures of 35 °C/27 °C. The same heat exchangers have to work in heating mode, considering an internal condenser unit thermal power of 2.58 kW and an external evaporator unit thermal power of 1.97 kW, for fixed ambient/indoor temperatures of 7 °C/20 °C.

Regarding the model calibration, for the compressor and the thermostatic valve, both sub-models have been calibrated on manufacturer data. Regarding heat exchanger and faults instead, well known and used correlation of the literature and phenomenological relation are employed. Due to the novelty of this work, a validation of the entire system model is not possible. However, with the aim of this work to analyse trends related to the occurring of faults, and not to focus on the precise numerical data, we considered this approach reasonable.

5. Results: Effect of faults on the thermodynamic cycle

It is important to define the most influenced measurable parameters to develop FDDE strategies, analysing their effect on the thermodynamic cycle. By imposing the faulty conditions, the resolution of the implemented model equations previously described

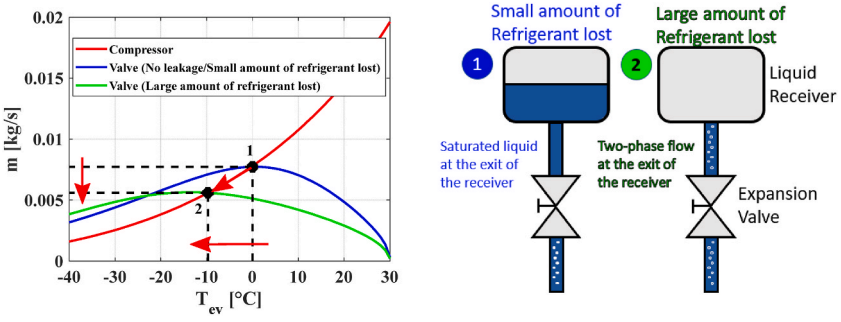

Fig. 3. Example of the valve behaviour in case of a liquid receiver of presence ($x_{in,valve} = 0$, blue line) and absence ($x_{in,valve} = 0.2$, green line) of refrigerant charge in the liquid receiver). (For interpretation of the references to colour in this figure legend, the reader is referred to the Web version of this article.)

Table 1
Rated parameters of the system investigated and geometrical characteristics of the internal and external heat exchangers.

Parameter	Machine	
Heating Capacity (7–20 °C) [kW]	2.58	
Working fluid	R32	
Rated evaporator superheating (°C)	7.0	
Liquid line length (m)	0.5	
Rated refrigerant charge (g)	490	
Compressor rated speed (rpm)	1140	
	Internal Unit	**External Unit**
Dimensions [m] (Length x Width x Height)	0.55 × 0.17 x 0.16	0.8 × 0.4 x 0.51
Number of circuits – rows – tubes per row	4–9 – 8	4–2 – 26
Longitudinal tube pitch [m]	0.02	0.02
Transverse tube pitch [m]	0.02	0.02
Fin pitch [mm]	2	2
Fin thickness [mm]	0.3	0.3
Tube diameter [mm]	7	7
Tube thickness [mm]	0.5	0.5
Tube thermal conductivity [$Wm^{-1}K^{-1}$]	386 (Copper)	
Fin thermal conductivity [$Wm^{-1}K^{-1}$]	204 (Aluminum)	

provides all the corresponding thermodynamic cycle parameters such as evaporation and condensation pressures and temperatures, suction and discharge temperature of the compressor, thermal and electrical powers and COP. For instance, regarding standalone faults, Fig. 4 shows three T-s diagrams in case of a 40% condenser fouling (Fig. 4(a)), a 40% evaporator fouling (Fig. 4(b)) and a 30% refrigerant leakage (Fig. 4(c)). Faulty thermodynamic cycles, represented by dashed lines, are compared with the fault-free cycle represented by solid lines, both in terms of thermodynamic conditions of refrigerant and of the two secondary fluids temperatures at the condenser and at the evaporator, for fixed conditions of ambient and indoor temperatures of respectively 7 °C and 20 °C.

In case of a 40% condenser fouling (Fig. 4(a)), the most influenced variable is the condensing temperature, which increases of about 7 °C compare with the fault-free case, whereas the outlet compressor temperature and air condenser temperature difference increase respectively of about 17 °C and 12.5 °C. On the other hand, both evaporating temperature and evaporator air temperature difference seem to be almost unaffected. These aspects result in a COP degradation of about 16%, and a heating capacity which remains almost unchanged. These results are comparable with the ones obtained in our previous work for the cooling mode [1], in which the COP penalization was about 13%. In case of a 40% evaporator fouling (Fig. 4(b)), it does not particularly affect the thermodynamic cycle, except for the evaporator fouling which seems to decrease of approximately 2 °C. It reflects on a reduction in heating capacity of about 4%, and a COP penalization of approximately 3.2%, which is quite lower compared to the one obtained for the cooling mode of approximately 17%. Finally, in case of a 30% refrigerant leakage (Fig. 4(c)), both evaporating and condensing temperatures decrease

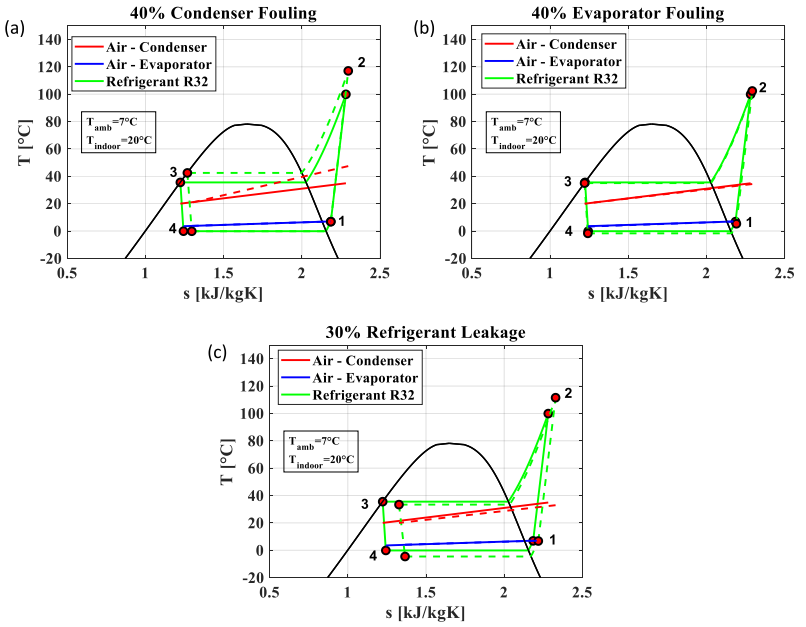

Fig. 4. Temperature – specific entropy diagrams comparison between faulty (dashed lines) and fault-free (solid lines) conditions, in case of a 40% condenser fouling (a), a 40% evaporator fouling (b) and a 30% refrigerant leakage (c), for fixed conditions of ambient and indoor temperature of respectively 7 °C and 20 °C.

respectively of 1.8 and 2.3 °C. Outlet compressor temperature and outlet evaporator superheating increase of about 13 °C and 5 °C respectively, compared with the fault-free case, whereas air temperature differences are slightly affected by this fault, with a 0.6 °C reduction at the evaporator and a 2.1 °C reduction at the condenser. Ultimately, a heating capacity reduction of approximately 21.3%, and a COP reduction of about 12% are obtained. A slightly higher performance degradation (14%) was obtained in cooling mode from our previous work [38], whereas the capacity reduction was slightly lower (15%).

The combination of more than one occurring fault can cause an overlapping effect on measured parameters of the machine thermodynamic cycle, causing an enhancement or a mitigation. Therefore, the effects of two and three faults combination are analysed in Fig. 5, by analysing and comparing faulty conditions characterized by a 40% condenser fouling (Fig. 5(a)), 40% evaporator fouling (Fig. 5(b)) and 30% refrigerant leakage (Fig. 5(c)) respectively, both standalone and combined in pairs. Fig. 5(d) instead compares the thermodynamic conditions related to the combination of all the three faults investigated with the fault-free case.

By combining a 40% condenser fouling and a 40% evaporator fouling, evaporating temperature decrease of about 1 °C compared with a standalone condenser fouling, whereas the condensing temperature increase is slightly mitigated, passing from 7 °C to 6.4 °C. On the other hand, the outlet compressor temperature increase is enhanced (+18.6 °C) compared with standalone faulty conditions, whereas air temperature differences remain almost unaffected by the combination of faults compared with an only condenser fouling. This results in a heating capacity which remains unchanged compared with an only evaporator fouling, whereas the performance degradation of 17.5% is higher compared to the two standalone faulty conditions investigated.

By combining instead a 40% condenser fouling and a 30% refrigerant leakage, this causes a higher decrease of the evaporating temperature of approximately 3 °C compared with a standalone condenser fouling and slightly lower than an only refrigerant leakage. Regarding condensing temperature and air temperature difference at the condenser, the contrasting effect of the two faults investigated causes a mitigation in the increase of these two variables, which rises respectively of 4.8 °C and 10.0 °C against the 7 °C and 12.5 °C increase of a standalone condenser fouling. Moreover, the increase of evaporator superheating is slightly mitigated compared to a standalone refrigerant leakage, passing from approximately 4.7 °C–2.6 °C. Finally, the heating capacity reduction results to be mitigated compared with an only refrigerant leakage, of about 12%, whereas the COP penalization is of approximately 21%, so enhanced by the contemporaneity of the two faults.

By combining a 40% evaporator fouling and a 30% refrigerant leakage, the evaporating and condensing temperature reductions are both enhanced by the overlapping effect of the two faults, becoming respectively 6 °C and 3 °C lower than the fault-free case. The outlet compressor temperature and the evaporator superheating increase of about respectively 14.3 °C and 5 °C, causing a reduction of

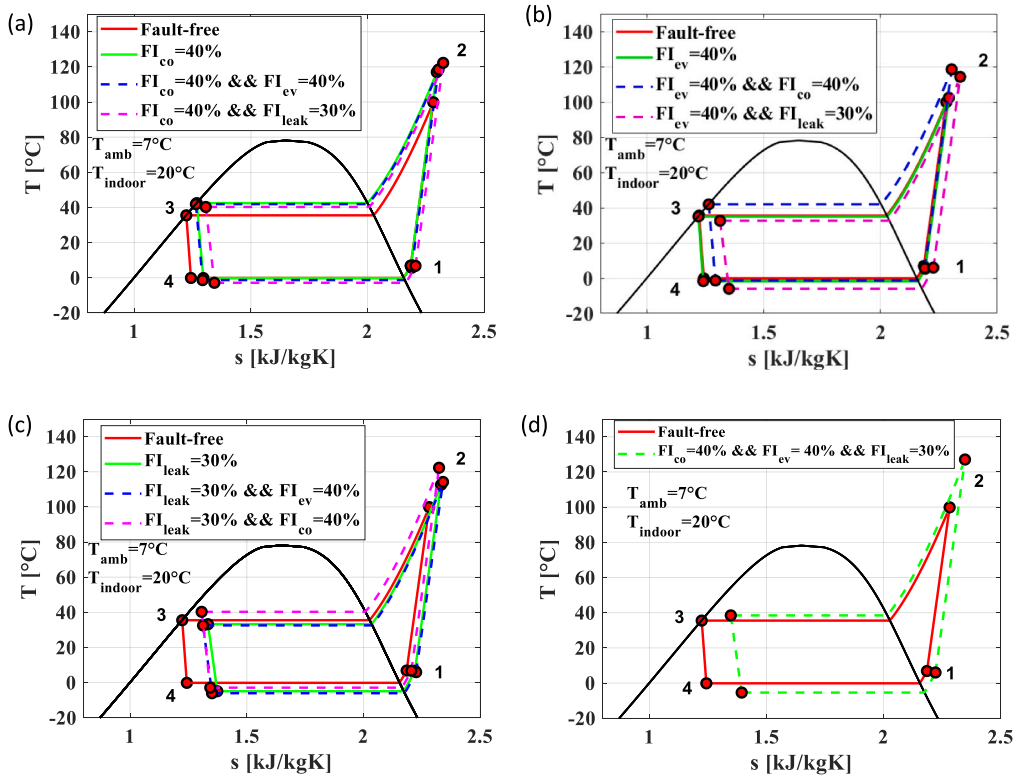

Fig. 5. Temperature-specific entropy diagrams for fault-free (solid red lines), standalone faulty (green solid lines) and simultaneous faulty (dashed lines) conditions, for ambient and indoor temperatures of 7 °C and 20 °C, in case of a 40% condenser fouling(a), 40% evaporator fouling(b) and 30% refrigerant leakage (c) standalone and combined in pairs, and in case of all the three faults simultaneously combined (d). (For interpretation of the references to colour in this figure legend, the reader is referred to the Web version of this article.)

heating capacity and COP of respectively 22.5% and 15.6%, both higher than the degradations obtained for the standalone faults.

Finally, by combining all the three faults investigated, so a 40% condenser fouling, a 40% evaporator fouling and a 30% refrigerant leakage, it can be noticed a 5.3 °C evaporating temperature reduction caused by evaporator fouling and refrigerant leakage and a 3 °C condensing temperature increase caused by the predominance of the condenser fouling effect on the others. Outlet compressor temperature increases of about 27 °C, and all these aspects cause a heating capacity and COP reduction of respectively 21.3% and 25.8%.

All the numerical results in terms of evaporating and condensing temperatures, outlet compressor temperature, outlet evaporator superheating, air temperature differences at the evaporator and condenser, heating capacity and COP are reported in Table 2, for the fault-free, standalone and combined faulty conditions. Differences with the fault free cases are reported for each variable in brackets.

6. Results: Performance maps

Results of COP depending on the fault intensity value are reported in Fig. 6, for respectively condenser fouling (Fig. 6(a)), evaporator fouling (Fig. 6(b)) and refrigerant leakage (Fig. 6(c)), and for a fixed indoor temperature of 20 °C. As expected, COP values in heating mode decrease both with the decrease of the external temperature and with the rise of the three fault intensities. Regarding the internal condenser fouling, the decrease of COP with fault intensity slight increase for higher fault intensities, with a more evident effect observable for higher ambient temperatures. On the other hand, the external evaporator fouling seems to slightly affect the system performances, with the COP degradation almost not influenced by fouling for lower temperatures, and slightly linearly increasing for higher external temperatures. Finally, the refrigerant leakage seems to slightly affect the system performance for low values of fault intensity, due to the effect of liquid receiver, with a COP degradation that strongly increases for refrigerant leakages higher than 30%. Overall, comparing results with the one obtained for the cooling mode, the effect of performance degradation in heating mode is almost the same for refrigerant leakage and condenser fouling, whereas the effect of evaporator fouling is much more marginal.

For multiple simultaneous faults instead, the COP penalization values are reported in Fig. 6(d), depending on the fault intensities for the three faults investigated, occurring simultaneously in groups of two or three, in fixed conditions of ambient and indoor temperatures of 7 °C and 20 °C. $COP_{penaliz}$ has been defined as follows:

$$COP_{penaliz} = \frac{COP_{fault-free} - COP_{faulty}}{COP_{fault-free}} \bullet 100 \tag{14}$$

The lower effect of the evaporator fouling in heating mode, compared to the one encountered for the cooling mode, is related to the fact that the external unit, which has been designed as a condenser in cooling mode, results to be oversized for the heating mode, where the thermal power transferred is lower due to similar thermal capacities of both operating conditions (approximately 2.6 kW). In Table 3 results in terms of evaporation and condensation temperatures, COP, heat exchanger thermal powers and global conductances are shown, comparing a fault-free and a 30% evaporator fouling conditions. In this case, it is worth noting that, despite a reduction of the global conductance of respectively the internal and external unit in cooling and heating modes, the external unit thermal power of the heating mode is approximately the half of the one of the cooling mode, passing from 3.31 to 1.99 in fault-free conditions.

This aspect can be better observed also in the following figures, in which results in terms of COP and $\dot{Q}_{ev}$ penalization caused by fouling are reported as a function of the average temperature difference at the evaporator, for both the operating modes and for several evaporator fouling fault intensities. It is worth noting that the slight COP penalization for the heating mode corresponds to a lower exchanger thermal power at the evaporator, and to lower average temperature differences, compared to the cooling mode, as shown in Fig. 7(a). Same concerns are also valid regarding the penalization of the evaporator thermal power itself, as shown in Fig. 7(b).

Table 2
Values assumed by evaporating, condensing and outlet compressor temperatures, outlet evaporator superheating, air temperature differences at the evaporator and condenser, heating capacity and COP, for all the standalone and simultaneous faulty conditions investigated.

Operation (Difference with fault-free)	T_{ev} [°C]	T_{co} [°C]	$T_{out,comp}$ [°C]	ΔT_{sh} [°C]	$\Delta T_{air,ev}$ [°C]	$\Delta T_{air,cond}$ [°C]	$\dot{Q}_{co}$ [kW]	COP
Fault-free	−0.1	35.5	99.9	7.0	3.5	14.9	2.58	4.35
40% Condenser Fouling	−0.2	42.5	117.0	7.0	3.3	27.4	2.56	3.65
	(−0.1 °C)	(+7.0 °C)	(+17.1 °C)	(+0.0 °C)	(−0.2 °C)	(+12.5 °C)	(−0.8%)	(−16.1%)
40% Evaporator Fouling	−1.7	35.0	102.3	7.0	3.8	14.3	2.48	4.21
	(−1.6 °C)	(−0.5 °C)	(+2.4 °C)	(+0.0 °C)	(+0.3 °C)	(−0.6 °C)	(−3.9%)	(−3.2%)
30% Refrigerant Leakage	−4.9	33.2	112.6	11.7	2.9	12.8	2.03	3.84
	(−4.8 °C)	(−2.3 °C)	(+12.7 °C)	(+4.7 °C)	(−0.6 °C)	(−2.1 °C)	(−21.3%)	(−11.7%)
40% Condenser Fouling + 40% Evaporator Fouling	−1.3	41.9	118.5	7.0	3.6	26.7	2.48	3.59
	(−1.2 °C)	(+6.4 °C)	(+18.6 °C)	(+0.0 °C)	(+0.1 °C)	(+11.8 °C)	(−3.9%)	(−17.5%)
40% Condenser Fouling + 30% Refrigerant Leakage	−2.9	40.3	122.3	9.6	2.9	24.9	2.27	3.44
	(−2.8 °C)	(+4.8 °C)	(+22.4 °C)	(+2.6 °C)	(−0.6 °C)	(+10.0 °C)	(−12.0%)	(−20.9%)
40% Evaporator Fouling + 30% Refrigerant Leakage	−6.1	32.5	114.2	12.0	3.0	12.0	2.00	3.67
	(−6.0 °C)	(−3.0 °C)	(+14.3 °C)	(+5.0 °C)	(−0.5 °C)	(−2.9 °C)	(−22.5%)	(−15.6%)
40% Condenser Fouling + 40% Evaporator Fouling + 30% Refrigerant Leakage	−5.4	38.5	127.1	11.4	2.9	22.9	2.03	3.23
	(−5.3 °C)	(+3.0 °C)	(+27.2 °C)	(+4.4 °C)	(−0.6 °C)	(+8.0 °C)	(−21.3%)	(−25.8%)

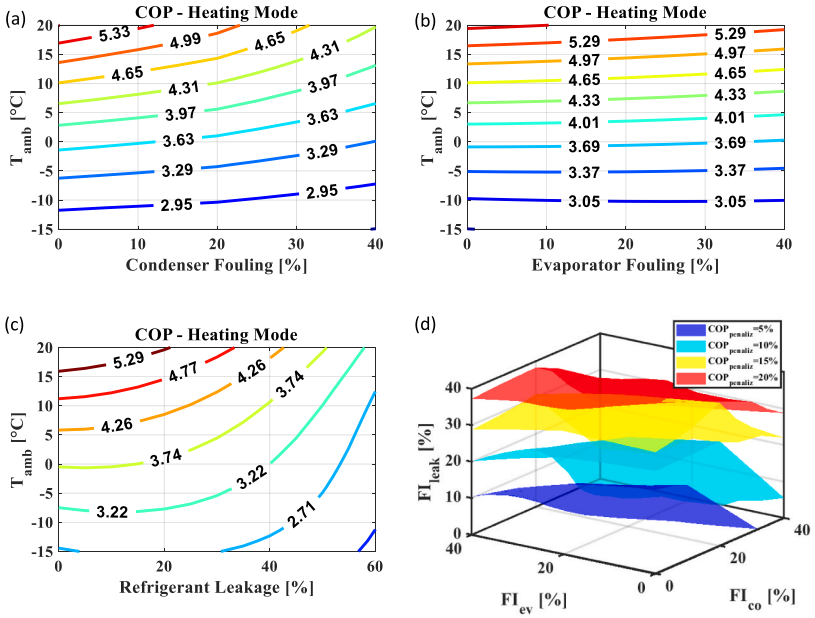

Fig. 6. COP maps depending on the ambient temperature and the fault intensity value, in case of condenser fouling (a), evaporator fouling (b) and refrigerant leakage (c) for an indoor temperature of 20 °C. Iso-performance degradation ($COP_{penaliz}$) maps depending on the three fault intensities (d), for fixed ambient and indoor temperature of respectively 7 °C and 20 °C.

Table 3
Comparisons in terms of evaporation and condensation temperatures, COP, heat exchangers thermal powers and global conductances between results obtained for the cooling and heating modes.

	Cooling (Summer)		Heating (Winter)	
Ambient Temperature [°C]	35 °C		7 °C	
Indoor Temperature [°C]	27 °C		20 °C	
	Fault-free	FI_{ev} = 30%	Fault-free	FI_{ev} = 30%
Evaporation Temperature [°C]	10.8	6.7	−0.1	−1.2
Condensation Temperature [°C]	45.1	44.4	35.5	35.2
COP	3.65	3.20	4.35	4.26
External unit thermal power [kW]	3.31	3.01	1.99	1.93
Internal unit thermal power [kW]	2.60	2.29	2.58	2.52
External unit global conductance [W/K]	368	343	413	335
Internal unit global conductance [W/K]	565	506	249	244

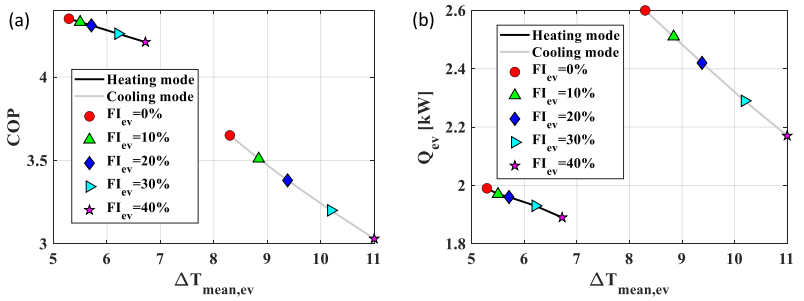

Fig. 7. COP (a) and evaporator thermal power (b) as a function of the mean temperature difference between air and refrigerant at the evaporator, obtained for an evaporator fouling fault intensity ranging from 0% to 40%, and for both the heating and cooling operating modes.

Therefore, all these considerations lead to a lower effect of the heat transfer surface penalization caused by fouling.

7. Results: Seasonal simulations

The system analysed has been dynamically simulated, along a lifetime period of 12 years, in order to analyse the effect of faults on the seasonal performance and on the environmental impact. Regarding the user for which the investigated machine is operating, a room with an average global conductivity of 55 W/K has been considered, evaluated according to the European Regulation (EU) 2016/2281 [43] in order to have a machine able to guarantee the user load at least for the 98% of the working hours, with a bivalent temperature of −10 °C. Different scenarios in terms of fault intensity evolution, maintenance strategy and climate conditions have been considered. In terms of occurring faults, different scenarios are obtained combining the following fault intensities.

- Ideal case: referred to a fault-free scenario, without the presence of any condenser fouling, evaporator fouling and refrigerant leakage
- Refrigerant leakage (RL). Values for refrigerant leakage of 20% per year ($RL_{max} \cong 98$ g/year), 10% per year (½ RL_{max}) and 5% per year (¼ RL_{max}) have been considered. The maximum value is chosen according to typical values of refrigerant leakages of this kind of air conditioning appliances, according to IIR [44]. Since the system pipeline is always characterized by a higher pressure than the external environment, the refrigerant leakage evolution has been considered linear with the machine lifetime, independently from if the machine is operating or not.
- Condenser fouling (CF). Heat exchanger fouling development has been considered with a hyperbolic tangent trend depending on the number of years. As a matter of fact, according to experimental evidences [45], fouling evolution is characterized by an initial higher deposition process, and by a growth rate that becomes lower and asymptotic when deposition and removal rates become equivalent each other, up to a maximum fault intensity. Therefore, values for condenser fouling of 40% (CF_{max}), 20% (½ CF_{max}) and 10% (¼ CF_{max}) have been considered. Similar values have been adopted by several other works of the literature [21,46]. Moreover, the fouling accumulation has been considered only if the machine is operating, with a number of hours to reach the 90% of the maximum level of fouling of 5000.
- Evaporator fouling (EF). The same hypotheses of condenser fouling in terms of fault evolution along time have been adopted. Therefore, values for evaporator fouling of 40% (EF_{max}), 20% (½ EF_{max}) and 10% (¼ EF_{max}) have been considered, similar to the ones adopted by other works of the literature. Also in this case the fouling process has been considered growing only if the machine is operating, with a number of working hours of 3000 to reach the 90% of the maximum level of fouling. It is worth noting that this number is lower than the one fixed for the condenser, because a higher fouling growth rate is expected for the external unit than the internal.

In terms of maintenance strategies, the following have been considered.

- Not planned maintenance by the user. The maintenance operation for every kind of fault occurs only when the user realizes about the presence of a faulty condition due to a lack of service. Numerically, every fault is solved whenever the machine is not able to satisfy neither the 30% of the thermal load requested by the user.
- Ordinary maintenance every 4 years. After each 4 year period every fault is solved.
- Ordinary maintenance every 2 years. After each 2 year period every fault is solved.
- Ordinary maintenance every year. After each 1 year period every fault is solved.

Finally, this investigation has been carried out for the three climate conditions of Vienna in Austria, New York in USA and Beijing in China. These three cities have been chosen because their high request of thermal load in winter can accurately describe the behaviour of the machine considered in this work. In all cases the heating season has been considered between the months of October and April. Values for the number of working hours of these climates depending on the external ambient temperature, and ambient temperature evolution along the winter months are reported in Fig. 8. It can be noticed that Vienna is characterized by a tight distribution of number of hours in which ambient temperature is between 0 and 20 °C, New York by a slightly larger distribution, with both cities characterized by the same minimum temperatures. The city of Beijing instead is characterized by the lowest minimum temperatures compare

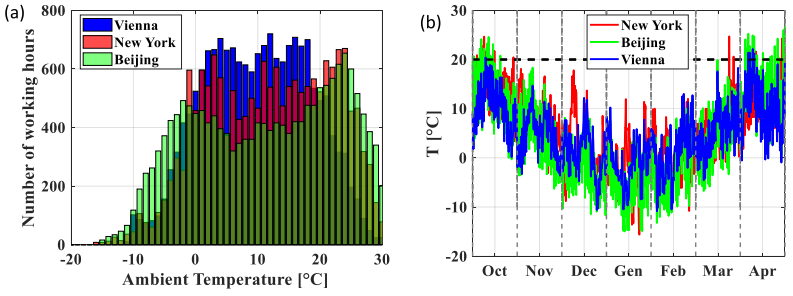

Fig. 8. Number of working hours vs. ambient temperature (a) and ambient temperature evolution along the heating season (b) in the three climate conditions investigated of New York, Beijing and Vienna.

Table 4
Number of working hours in which the ambient temperature drops below 20 °C, for the climate conditions investigated.

Number of Working Hours ($T_{amb} < 20°C$)		
New York	Beijing	Vienna
6387	5967	7613

with other climate conditions; however the temperature distribution seems to be the largest compared to the others.

Considering the machine working whenever the ambient temperature drops below 20 °C, Table 4 shows the number of working hours for the three climate conditions investigated. It can be noticed that Vienna is characterized by the highest number of hours, Beijing by the lowest (despite the lowest values of ambient temperatures) and New York by an intermediate value between Vienna and Beijing.

A total of 768 scenarios has been simulated by combining all the possible options mentioned before, and for each of them values of seasonal coefficient of performance (SCOP) and total equivalent warming impact (TEWI) are evaluated. SCOP is defined in this case as the total heating energy delivered to the user divided by the total electric energy used to activate compressor and auxiliaries of the machine. TEWI instead is defined as the sum of two contributions, the direct CO_2 emissions related to the refrigerant leakages from the system pipeline, and the indirect related to the energy consumption of the machine. Both are evaluated with the following expressions.

$$SCOP = \frac{\sum_{t=1}^{n} Q_{user,t}}{\sum_{t=1}^{n} W_{el,t}} = \frac{\sum_{t=1}^{n} Q_{user,t}}{\sum_{t=1}^{n} \frac{Q_{user,t}}{COP_t}} \tag{15}$$

$$TEWI = m_{leak} \bullet GWP + W_{el,tot} \bullet f_{ee} \quad \left(kgCO_{2,equiv}\right) \tag{16}$$

m_{leak} is the mass of refrigerant leaked along the entire machine lifetime, and it depends on the faulty scenario considered, whereas f_{ee} is the average emission factor for the electricity production and it depends on the country of the climate condition investigated. COP values dependency with the rotational speed of the compressor has been neglected in this work.

Fig. 9 shows results considering a 10%/year refrigerant leakage, a maximum condenser fouling of 10% and a maximum evaporator fouling of 20%, for New York climate conditions and in case of a not-planned (Fig. 9(a)) and every 2 years (Fig. 9(b)) maintenance scenarios. On the top part of each image COP evolution along the entire machine lifetime is shown, distinguishing red points related to the faulty conditions from grey points corresponding to the fault-free case. On the bottom part of each image instead the corresponding fault evolution is presented for each of the three kinds of faults investigated. It is worth noting that, if no maintenance operation is planned in these conditions, the user realizes about the presence of the fault only after about 9 years, where values of SCOP become lower than 1 (COP values in the fault-free condition are between 3 and 6). Higher values of COP are instead obtained in case of an every two year maintenance scenario, with a seasonal coefficient of performance which increases of about 33% passing from 2.92 to 3.88, therefore closer to the ideal scenario (SCOP of the ideal scenario is 3.98).

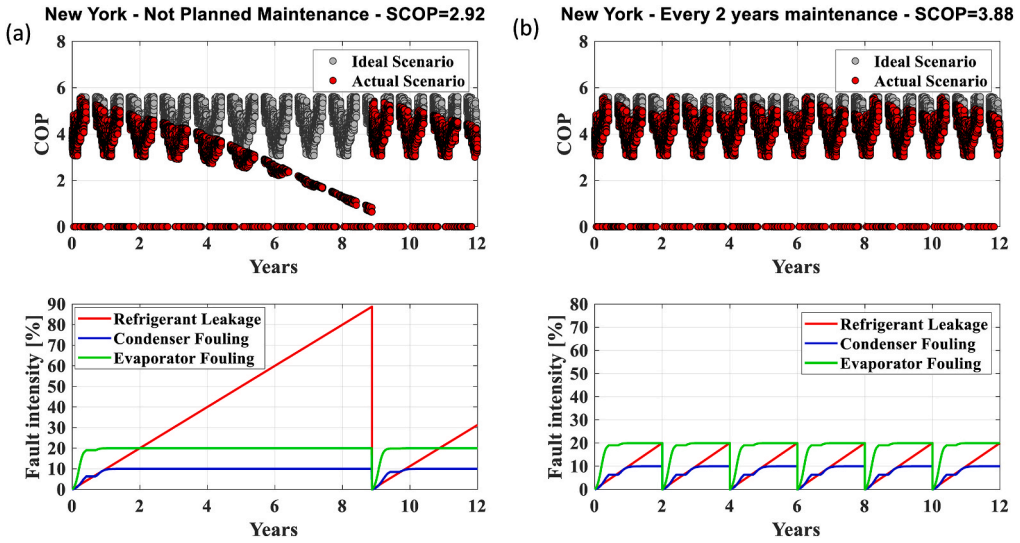

Fig. 9. COP values (upper part of figures) and related fault intensity evolutions (lower part of figures) along a 12 year lifetime of the heat pump investigated, in case of a refrigerant leakage of 10%/year, a maximum condenser and evaporator fouling of respectively 10% and 20%, in New York climate conditions, for a fixed indoor temperature of 20 °C, and in case of a not-planned (a) and every 2 year maintenance strategy.

Table 5
Values of SCOP, TEWI and number of maintenance interventions extracted from tables in the appendix, obtained considering the fault-free case (test 1) and the scenarios in which every fault is occurring standalone with its maximum fault intensity (tests 4, 13 and 49), for New York climate conditions.

Test	Fault Evolution			New York		
	RL	CF	EF	SCOP	TEWI [$t_{CO2.equiv}$]	Ninterv.
1	0	0	0	3.98	6.19	0
Not planned maintenance by User						
4	0	CFmax	0	3.46	7.13	0
13	0	0	EFmax	3.90	6.32	0
49	RLmax	0	0	2.98	8.27	2
Ordinary maintenance every 4 years						
4	0	CFmax	0	3.51	7.03	3
13	0	0	EFmax	3.91	6.31	3
49	RLmax	0	0	2.99	8.81	3
Ordinary maintenance every 2 years						
4	0	CFmax	0	3.59	6.87	6
13	0	0	EFmax	3.92	6.30	6
49	RLmax	0	0	3.83	7.23	6
Ordinary maintenance every year						
4	0	CFmax	0	3.75	6.58	12
13	0	0	EFmax	3.93	6.27	12
49	RLmax	0	0	3.97	7.01	12

Results of all the simulations are provided in several tables in the appendix of this paper. Table 5 is an extract of all the results in which values of SCOP, TEWI and number of interventions are reported for New York climate condition and for standalone faults characterized by the maximum fault intensity. It is worth noting that, in case of a not planned maintenance scenario, SCOP results 13%, 2% and 25% penalized for respectively a maximum condenser fouling, evaporator fouling and refrigerant leakage. By considering an ordinary maintenance every 4 years, both the number of maintenance and SCOP values increase. However, in case of refrigerant leakage at least an ordinary maintenance every two years is able to increase SCOP which becomes only 4% lower than the ideal case, whereas in case of condenser fouling at least a 1 year maintenance operation is necessary to guarantee a SCOP which becomes 6% lower than the fault-free scenario. Similar consideration could be done for TEWI results, which values becomes closer to the ideal case by increasing the number of maintenance interventions.

Regarding the effect of climate, in case of fault-free conditions, SCOP values for New York and Vienna are the same, whereas it is lower for Beijing, due to the lowest level of external temperatures, as shown in the complete results reported in appendix. However, the effect of fault penalization strongly depends on the working hours in which the machine is operating in non proper conditions, a number which is higher for New York and Vienna, and lower for Beijing. Therefore, it explains the fact that the SCOP differences between cities tends to reduce in case of faulty conditions in a not-planned maintenance scenario, and the fact that ordinary

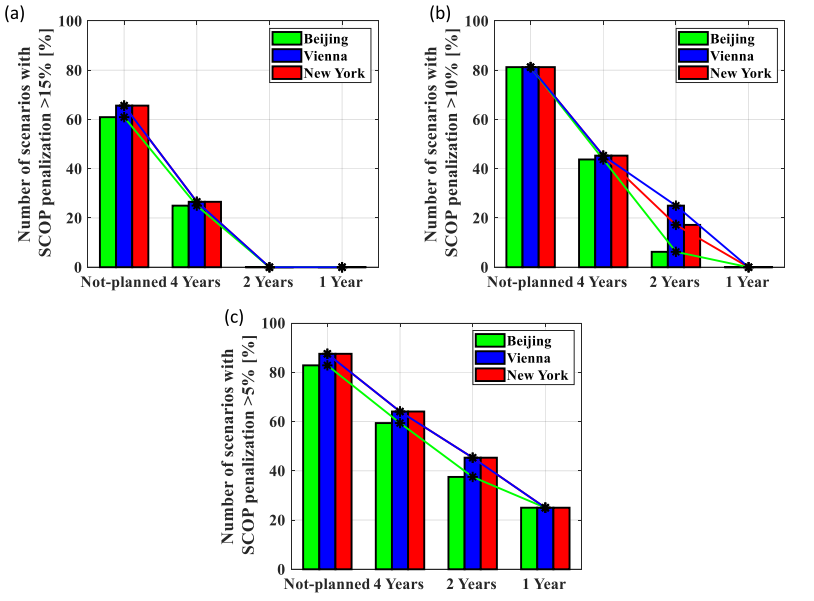

Fig. 10. Percentage of the 64 simulated scenarios, with a SCOP penalization over 15%(a), 10%(b) and 5%(c), depending on the maintenance strategy and on the climatic condition investigated.

maintenance strategies seem to be more convenient for cities characterized by a higher number of working hours.

Finally, percentages of the 64 scenarios with a SCOP penalization of 15%, 10% and 5% are reported respectively in Fig. 10(a), Fig. 10(b) and (c), depending on the climate condition and on the maintenance strategy considered. From Fig. 10(a) it is worth noting that with a not-planned maintenance, the scenarios with a SCOP penalization over 15% are approximately the 60% of the total, for all the climate conditions investigated. The percentages decrease to 20% and to almost 0% passing to a 4-year and 2-year maintenance scenario respectively. From Fig. 10(b) instead, it can be noticed that passing from a 4-year to a 2-year maintenance strategy, the number of scenarios which SCOP is penalized over 10% becomes almost 5% in case of Beijing, 22% for Vienna and 18% for New York. Finally, considering SCOP penalization over 5% (Fig. 10(c)), even with a yearly maintenance scenario, the minimum threshold of penalized scenario is about 20% for all the climate conditions investigated.

In cooling mode [1] we also obtained a high reduction of the penalized scenarios in increasing the number of maintenance interventions along the machine lifetime, in the investigated climate conditions of Miami, Naples and Shanghai. As a matter of fact, in that case, an every 2-year maintenance scenario was able to reduce the scenarios with a SCOP penalization over 10%, from 85% of the total to approximately 58% for Miami, 38% for Shanghai and 18% for Naples, whereas a maintenance operation every year guaranteed a reduction of the penalized scenarios to about 15% for Miami and to 0% for Naples and Shanghai.

Results show that it is not possible to identify a unique maintenance strategy able to reduce the number of penalized scenarios in the same way for all the climate conditions, as also obtained for the cooling mode [1]. Moreover, it should be noted that, considering an operating stock of machines, it is impossible to know in advance the fault probability curves on the single heat pump, since it depends on several non-controllable factors. Therefore, it would be useful to have an intelligent fault detection, diagnosis and evaluation (FDDE) method based on the machine monitoring, that would allow to carry out a maintenance intervention at the appropriate time, depending on the effective performance degradation. The proof of concept of this aspect have been demonstrated in a previous paper (Pelella et al. [38]).

8. Conclusions

This manuscript deals with a numerical investigation of a 2.6 kW air-to-air heat pump for residential heating. The analysis aims to recognize the effect of the three different typical soft faults of condenser fouling, evaporator fouling and refrigerant leakage on the system performance and the measured parameters of the thermodynamic cycle. Moreover, the machine has been dynamically simulated to estimate the effect of faults on seasonal performance and environmental impact, considering different fault intensity evolutions in 12 years of machine operation, different maintenance strategies among not-planned and organized every 4, 2 and 1 year, and three different climate conditions of New York, Beijing and Vienna. The main highlights are here reported.

- Several sub-models for the system components, and for the three faults investigated have been developed and put together in order to simulate the behaviour of the entire system
- Regarding the effect of faults on performances, COP decreases with the increase of fault intensities, whereas increases with the external ambient temperature. For condenser fouling and refrigerant leakage, the COP penalization is higher for higher ambient temperature, whereas it is almost negligible in case of evaporator fouling.
- A standalone 40% condenser fouling mostly influences the condensing temperature, which rises of about 7 °C compared with the fault free case, whereas a standalone 40% evaporator fouling slightly affects the evaporating temperature which decreases of about 2 °C. A standalone 30% refrigerant leakage instead causes a decrease of both evaporating and condensing temperature, an outlet evaporator superheating and an outlet compressor temperature increase. In these three cases, COP penalization is respectively 16%, 3% and 12% compared with the fault-free case. In cooling mode, instead, whose results are reported in our previous work [38], the COP penalization for the three investigated faults were approximately 13%, 17% and 14%. Therefore, penalizations caused by refrigerant leakage and condenser fouling are rather similar between the two operating modes, whereas the evaporator fouling seems to affect performance more in cooling mode. This aspect is mostly related to the fact that the external unit is designed in cooling mode as a condenser. Since the heating and cooling capacities of the internal unit are similar under different conditions (7 °C/20 °C for the heating mode and 35 °C/27 °C for the cooling mode), the external unit in winter has to handle a lower evaporating power compared to the cooling mode. The unit itself results to be oversized, and a heat transfer surface portion becomes useless for the evaporation, differently from the cooling mode in which all the heat transfer surface is employed in the condensation process. Therefore, a heat transfer surface penalization less than 40–50% in heating mode may lead to negligible effects on the thermodynamic cycle.
- From seasonal simulations, results show that SCOP results 13%, 2% and 25% penalized respectively for a maximum condenser and evaporator fouling of 40%, and 10%/year refrigerant leakage. In cooling mode instead a penalization of respectively 14%, 13% and 41% for the same fault intensity evolutions had been obtained.
- The employment of ordinary maintenance scenarios seems to be more effective for cities with a higher number of operating hours, for which the impact of faults on energy consumption is fundamental. Finally, a 4-year maintenance strategy is able to reduce to approximately 40% the number of scenarios which SCOP is penalized over 10%, whereas a 2-year strategy reduces this percentage to approximately 5% for Beijing, to 22% for Vienna and to 18% for New York.

Credit author statement

F. Pelella: Investigation, Data curation, Writing – Original draft. **L. Viscito**: Methodology, Formal Analysis, Writing – Review and Editing. **A.W. Mauro**: Conceptualization, Methodology, Resources, Supervision.

Declaration of competing interest

The authors declare that they have no known competing financial interests or personal relationships that could have appeared to influence the work reported in this paper.

Data availability

Data will be made available on request.

Appendix

Tables 6–9 shows the results in terms of SCOP, TEWI and of number of maintenance interventions, for all the scenarios obtained combining all the possible fault evolutions, climate conditions and maintenance strategies.

Table 6
Values of SCOP, TEWI and number of maintenance interventions depending on the fault intensity evolution and on the climate condition, in case of a not-planned maintenance by the user

Not planned maintenance by User												
Test	Fault Evolution			New York			Beijing			Vienna		
	RL	CF	EF	SCOP	TEWI [t_{CO2}]	Ninterv.	SCOP	TEWI [t_{CO2}]	Ninterv.	SCOP	TEWI [t_{CO2}]	Ninterv.
1	0	0	0	3.98	6.19	0	3.78	7.01	0	3.98	6.95	0
2	0	1/4 CFmax	0	3.88	6.36	0	3.69	7.17	0	3.88	7.13	0
3	0	1/2 CFmax	0	3.78	6.53	0	3.60	7.34	0	3.78	7.32	0
4	0	CFmax	0	3.46	7.13	0	3.33	7.94	0	3.46	8.00	0
5	0	0	1/4 EFmax	3.97	6.21	0	3.77	7.02	0	3.97	6.96	0
6	0	1/4 CFmax	1/4 EFmax	3.87	6.37	0	3.69	7.18	0	3.87	7.14	0
7	0	1/2 CFmax	1/4 EFmax	3.77	6.54	0	3.60	7.35	0	3.77	7.33	0
8	0	CFmax	1/4 EFmax	3.46	7.13	0	3.33	7.95	0	3.45	8.00	0
9	0	0	1/2 EFmax	3.97	6.22	0	3.77	7.03	0	3.96	6.98	0
10	0	1/4 CFmax	1/2 EFmax	3.87	6.38	0	3.68	7.19	0	3.86	7.16	0
11	0	1/2 CFmax	1/2 EFmax	3.77	6.55	0	3.60	7.36	0	3.76	7.35	0
12	0	CFmax	1/2 EFmax	3.46	7.14	0	3.33	7.95	0	3.45	8.01	0
13	0	0	EFmax	3.90	6.32	0	3.72	7.11	0	3.90	7.09	0
14	0	1/4 CFmax	EFmax	3.81	6.47	0	3.64	7.26	0	3.81	7.26	0
15	0	1/2 CFmax	EFmax	3.72	6.63	0	3.57	7.42	0	3.72	7.43	0
16	0	CFmax	EFmax	3.43	7.20	0	3.31	8.01	0	3.42	8.08	0
17	1/4 RLmax	0	0	3.51	7.21	0	3.39	7.98	0	3.50	8.08	0
18	1/4 RLmax	1/4 CFmax	0	3.44	7.35	0	3.31	8.15	0	3.44	8.22	0
19	1/4 RLmax	1/2 CFmax	0	3.37	7.50	0	3.23	8.33	0	3.37	8.38	0
20	1/4 RLmax	CFmax	0	3.13	8.04	0	3.05	8.81	0	3.13	9.02	0
21	1/4 RLmax	0	1/4 EFmax	3.49	7.25	0	3.37	7.99	0	3.48	8.12	0
22	1/4 RLmax	1/4 CFmax	1/4 EFmax	3.42	7.39	0	3.29	8.17	0	3.41	8.27	0
23	1/4 RLmax	1/2 CFmax	1/4 EFmax	3.34	7.55	0	3.22	8.36	0	3.34	8.44	0
24	1/4 RLmax	CFmax	1/4 EFmax	3.11	8.10	0	3.03	8.86	0	3.10	9.08	0
25	1/4 RLmax	0	1/2 EFmax	3.46	7.31	0	3.34	8.04	0	3.45	8.19	0

(*continued on next page*)

Table 6 (*continued*)

Not planned maintenance by User												
Test	Fault Evolution			New York			Beijing			Vienna		
	RL	CF	EF	SCOP	TEWI [t_{CO2}]	Ninterv.	SCOP	TEWI [t_{CO2}]	Ninterv.	SCOP	TEWI [t_{CO2}]	Ninterv.
26	1/4 RLmax	1/4 CFmax	1/2 EFmax	3.39	7.45	0	3.27	8.21	0	3.39	8.34	0
27	1/4 RLmax	1/2 CFmax	1/2 EFmax	3.32	7.61	0	3.19	8.41	0	3.32	8.50	0
28	1/4 RLmax	CFmax	1/2 EFmax	3.09	8.15	0	3.01	8.90	0	3.08	9.14	0
29	1/4 RLmax	0	EFmax	3.37	7.50	0	3.27	8.22	0	3.36	8.40	0
30	1/4 RLmax	1/4 CFmax	EFmax	3.31	7.63	0	3.20	8.39	0	3.30	8.54	0
31	1/4 RLmax	1/2 CFmax	EFmax	3.24	7.78	0	3.12	8.58	0	3.24	8.70	0
32	1/4 RLmax	CFmax	EFmax	3.03	8.30	0	2.95	9.04	0	3.02	9.30	0
33	1/2 RLmax	0	0	2.98	8.24	1	2.96	8.71	1	2.99	9.18	1
34	1/2 RLmax	1/4 CFmax	0	2.94	8.34	1	2.91	8.83	1	2.95	9.28	1
35	1/2 RLmax	1/2 CFmax	0	2.90	8.44	1	2.86	8.94	1	2.91	9.38	1
36	1/2 RLmax	CFmax	0	2.76	8.85	1	2.74	9.31	1	2.76	9.86	1
37	1/2 RLmax	0	1/4 EFmax	2.98	8.22	1	2.95	8.67	1	2.98	9.16	1
38	1/2 RLmax	1/4 CFmax	1/4 EFmax	2.93	8.34	1	2.90	8.81	1	2.94	9.28	1
39	1/2 RLmax	1/2 CFmax	1/4 EFmax	2.89	8.46	1	2.85	8.96	1	2.90	9.42	1
40	1/2 RLmax	CFmax	1/4 EFmax	2.75	8.87	1	2.73	9.34	1	2.75	9.89	1
41	1/2 RLmax	0	1/2 EFmax	2.96	8.26	1	2.93	8.72	1	2.97	9.21	1
42	1/2 RLmax	1/4 CFmax	1/2 EFmax	2.92	8.37	1	2.89	8.84	1	2.93	9.32	1
43	1/2 RLmax	1/2 CFmax	1/2 EFmax	2.87	8.50	1	2.84	8.99	1	2.88	9.45	1
44	1/2 RLmax	CFmax	1/2 EFmax	2.74	8.90	1	2.72	9.36	1	2.74	9.92	1
45	1/2 RLmax	0	EFmax	2.90	8.41	1	2.88	8.86	1	2.91	9.38	1
46	1/2 RLmax	1/4 CFmax	EFmax	2.86	8.52	1	2.84	8.98	1	2.87	9.48	1
47	1/2 RLmax	1/2 CFmax	EFmax	2.82	8.63	1	2.79	9.11	1	2.83	9.60	1
48	1/2 RLmax	CFmax	EFmax	2.73	8.89	1	2.70	9.37	1	2.74	9.92	1
49	RLmax	0	0	2.98	8.27	2	2.93	8.66	2	2.95	9.22	2
50	RLmax	1/4 CFmax	0	2.94	8.35	2	2.89	8.77	2	2.92	9.31	2
51	RLmax	1/2 CFmax	0	2.90	8.45	2	2.84	8.88	2	2.88	9.40	2
52	RLmax	CFmax	0	2.76	8.82	2	2.73	9.19	2	2.74	9.83	2
53	RLmax	0	1/4 EFmax	2.97	8.26	2	2.92	8.64	2	2.94	9.20	2
54	RLmax	1/4 CFmax	1/4 EFmax	2.93	8.37	2	2.88	8.76	2	2.91	9.31	2
55	RLmax	1/2 CFmax	1/4 EFmax	2.88	8.49	2	2.83	8.90	2	2.86	9.44	2
56	RLmax	CFmax	1/4 EFmax	2.75	8.85	2	2.72	9.22	2	2.73	9.87	2
57	RLmax	0	1/2 EFmax	2.95	8.31	2	2.91	8.68	2	2.92	9.26	2
58	RLmax	1/4 CFmax	1/2 EFmax	2.91	8.41	2	2.86	8.79	2	2.88	9.37	2
59	RLmax	1/2 CFmax	1/2 EFmax	2.86	8.53	2	2.81	8.94	2	2.84	9.49	2

(*continued on next page*)

Table 6 (*continued*)

Not planned maintenance by User												
Test	Fault Evolution			New York			Beijing			Vienna		
	RL	CF	EF	SCOP	TEWI [t_{CO2}]	Ninterv.	SCOP	TEWI [t_{CO2}]	Ninterv.	SCOP	TEWI [t_{CO2}]	Ninterv.
60	RLmax	CFmax	1/2 EFmax	2.74	8.89	2	2.71	9.25	2	2.71	9.91	2
61	RLmax	0	EFmax	2.89	8.47	2	2.85	8.82	2	2.86	9.43	2
62	RLmax	1/4 CFmax	EFmax	2.85	8.56	2	2.81	8.94	2	2.83	9.53	2
63	RLmax	1/2 CFmax	EFmax	2.82	8.66	2	2.76	9.07	2	2.79	9.64	2
64	RLmax	CFmax	EFmax	2.64	9.16	2	2.62	9.52	2	2.64	10.15	2

Table 7
Values of SCOP, TEWI and number of maintenance interventions depending on the fault intensity evolution and on the climate condition, in case of a 4 years ordinary maintenance strategy

Ordinary maintenance every 4 years												
Test	Fault Evolution			New York			Beijing			Vienna		
	RL	CF	EF	SCOP	TEWI [t_{CO2}]	Ninterv.	SCOP	TEWI [t_{CO2}]	Ninterv.	SCOP	TEWI [t_{CO2}]	Ninterv.
1	0	0	0	3.98	6.19	3	3.78	7.01	3	3.98	6.95	3
2	0	1/4 CFmax	0	3.89	6.34	3	3.70	7.15	3	3.89	7.11	3
3	0	1/2 CFmax	0	3.80	6.49	3	3.62	7.31	3	3.79	7.29	3
4	0	CFmax	0	3.51	7.03	3	3.37	7.84	3	3.50	7.89	3
5	0	0	1/4 EFmax	3.97	6.21	3	3.77	7.02	3	3.97	6.96	3
6	0	1/4 CFmax	1/4 EFmax	3.88	6.35	3	3.69	7.16	3	3.88	7.13	3
7	0	1/2 CFmax	1/4 EFmax	3.79	6.50	3	3.62	7.32	3	3.79	7.30	3
8	0	CFmax	1/4 EFmax	3.51	7.03	3	3.37	7.85	3	3.50	7.90	3
9	0	0	1/2 EFmax	3.97	6.22	3	3.77	7.03	3	3.96	6.98	3
10	0	1/4 CFmax	1/2 EFmax	3.88	6.36	3	3.69	7.17	3	3.87	7.14	3
11	0	1/2 CFmax	1/2 EFmax	3.79	6.51	3	3.61	7.32	3	3.78	7.31	3
12	0	CFmax	1/2 EFmax	3.50	7.04	3	3.37	7.85	3	3.50	7.91	3
13	0	0	EFmax	3.91	6.31	3	3.73	7.10	3	3.90	7.08	3
14	0	1/4 CFmax	EFmax	3.83	6.45	3	3.65	7.24	3	3.82	7.23	3
15	0	1/2 CFmax	EFmax	3.74	6.59	3	3.58	7.38	3	3.74	7.39	3
16	0	CFmax	EFmax	3.48	7.10	3	3.35	7.90	3	3.47	7.97	3
17	1/4 RLmax	0	0	3.97	6.41	3	3.77	7.22	3	3.97	7.16	3
18	1/4 RLmax	1/4 CFmax	0	3.88	6.55	3	3.69	7.36	3	3.88	7.32	3
19	1/4 RLmax	1/2 CFmax	0	3.79	6.70	3	3.62	7.51	3	3.79	7.49	3
20	1/4 RLmax	CFmax	0	3.51	7.23	3	3.37	8.04	3	3.50	8.09	3
21	1/4 RLmax	0	1/4 EFmax	3.96	6.43	3	3.76	7.23	3	3.96	7.18	3
22	1/4 RLmax	1/4 CFmax	1/4 EFmax	3.87	6.56	3	3.69	7.37	3	3.87	7.34	3
23	1/4 RLmax	1/2 CFmax	1/4 EFmax	3.79	6.71	3	3.61	7.52	3	3.78	7.51	3
24	1/4 RLmax	CFmax	1/4 EFmax	3.51	7.23	3	3.37	8.05	3	3.50	8.10	3
25	1/4 RLmax	0	1/2 EFmax	3.94	6.45	3	3.75	7.25	3	3.94	7.21	3

(*continued on next page*)

Table 7 (*continued*)

Ordinary maintenance every 4 years												
Test	Fault Evolution			New York			Beijing			Vienna		
	RL	CF	EF	SCOP	TEWI [t_{CO2}]	Ninterv.	SCOP	TEWI [t_{CO2}]	Ninterv.	SCOP	TEWI [t_{CO2}]	Ninterv.
26	1/4 RLmax	1/4 CFmax	1/2 EFmax	3.86	6.58	3	3.68	7.39	3	3.86	7.36	3
27	1/4 RLmax	1/2 CFmax	1/2 EFmax	3.78	6.73	3	3.61	7.53	3	3.77	7.53	3
28	1/4 RLmax	CFmax	1/2 EFmax	3.50	7.24	3	3.37	8.05	3	3.50	8.11	3
29	1/4 RLmax	0	EFmax	3.87	6.57	3	3.70	7.35	3	3.86	7.35	3
30	1/4 RLmax	1/4 CFmax	EFmax	3.81	6.68	3	3.64	7.47	3	3.80	7.47	3
31	1/4 RLmax	1/2 CFmax	EFmax	3.73	6.81	3	3.57	7.61	3	3.72	7.62	3
32	1/4 RLmax	CFmax	EFmax	3.47	7.30	3	3.35	8.11	3	3.46	8.18	3
33	1/2 RLmax	0	0	3.83	6.84	3	3.65	7.64	3	3.82	7.64	3
34	1/2 RLmax	1/4 CFmax	0	3.77	6.94	3	3.60	7.75	3	3.76	7.75	3
35	1/2 RLmax	1/2 CFmax	0	3.70	7.05	3	3.54	7.87	3	3.70	7.87	3
36	1/2 RLmax	CFmax	0	3.44	7.56	3	3.32	8.36	3	3.43	8.45	3
37	1/2 RLmax	0	1/4 EFmax	3.80	6.88	3	3.63	7.68	3	3.79	7.69	3
38	1/2 RLmax	1/4 CFmax	1/4 EFmax	3.75	6.98	3	3.58	7.79	3	3.74	7.80	3
39	1/2 RLmax	1/2 CFmax	1/4 EFmax	3.68	7.09	3	3.52	7.91	3	3.68	7.91	3
40	1/2 RLmax	CFmax	1/4 EFmax	3.43	7.59	3	3.31	8.39	3	3.42	8.49	3
41	1/2 RLmax	0	1/2 EFmax	3.77	6.94	3	3.61	7.73	3	3.76	7.75	3
42	1/2 RLmax	1/4 CFmax	1/2 EFmax	3.72	7.03	3	3.56	7.84	3	3.71	7.85	3
43	1/2 RLmax	1/2 CFmax	1/2 EFmax	3.66	7.14	3	3.50	7.95	3	3.65	7.96	3
44	1/2 RLmax	CFmax	1/2 EFmax	3.41	7.63	3	3.29	8.43	3	3.40	8.53	3
45	1/2 RLmax	0	EFmax	3.67	7.12	3	3.52	7.91	3	3.65	7.97	3
46	1/2 RLmax	1/4 CFmax	EFmax	3.63	7.20	3	3.48	8.00	3	3.62	8.04	3
47	1/2 RLmax	1/2 CFmax	EFmax	3.58	7.29	3	3.43	8.11	3	3.57	8.14	3
48	1/2 RLmax	CFmax	EFmax	3.35	7.75	3	3.24	8.55	3	3.34	8.68	3
49	RLmax	0	0	2.99	8.81	3	2.92	9.41	3	2.97	9.82	3
50	RLmax	1/4 CFmax	0	2.95	8.91	3	2.87	9.53	3	2.93	9.92	3
51	RLmax	1/2 CFmax	0	2.90	9.02	3	2.82	9.65	3	2.88	10.03	3
52	RLmax	CFmax	0	2.77	9.42	3	2.71	9.99	3	2.74	10.50	3
53	RLmax	0	1/4 EFmax	2.98	8.80	3	2.91	9.34	3	2.95	9.81	3
54	RLmax	1/4 CFmax	1/4 EFmax	2.93	8.93	3	2.86	9.50	3	2.91	9.94	3
55	RLmax	1/2 CFmax	1/4 EFmax	2.88	9.06	3	2.80	9.67	3	2.86	10.08	3
56	RLmax	CFmax	1/4 EFmax	2.75	9.45	3	2.70	10.02	3	2.73	10.54	3
57	RLmax	0	1/2 EFmax	2.96	8.85	3	2.89	9.39	3	2.93	9.86	3
58	RLmax	1/4 CFmax	1/2 EFmax	2.91	8.98	3	2.84	9.54	3	2.89	9.99	3
59	RLmax	1/2 CFmax	1/2 EFmax	2.86	9.11	3	2.79	9.71	3	2.85	10.14	3

(*continued on next page*)

Table 7 (*continued*)

Ordinary maintenance every 4 years												
Test	Fault Evolution			New York			Beijing			Vienna		
	RL	CF	EF	SCOP	TEWI [t_{CO2}]	Ninterv.	SCOP	TEWI [t_{CO2}]	Ninterv.	SCOP	TEWI [t_{CO2}]	Ninterv.
60	RLmax	CFmax	1/2 EFmax	2.74	9.50	3	2.68	10.05	3	2.71	10.59	3
61	RLmax	0	EFmax	2.90	9.01	3	2.84	9.54	3	2.87	10.04	3
62	RLmax	1/4 CFmax	EFmax	2.86	9.12	3	2.79	9.69	3	2.84	10.16	3
63	RLmax	1/2 CFmax	EFmax	2.82	9.24	3	2.74	9.83	3	2.80	10.28	3
64	RLmax	CFmax	EFmax	2.70	9.60	3	2.64	10.14	3	2.68	10.70	3

Table 8
Values of SCOP, TEWI and number of maintenance interventions depending on the fault intensity evolution and on the climate condition, in case of a 2 years ordinary maintenance strategy

Ordinary maintenance every 2 years												
Test	Fault Evolution			New York			Beijing			Vienna		
	RL	CF	EF	SCOP	TEWI [t_{CO2}]	Ninterv.	SCOP	TEWI [t_{CO2}]	Ninterv.	SCOP	TEWI [t_{CO2}]	Ninterv.
1	0	0	0	3.98	6.19	6	3.78	7.01	6	3.98	6.95	6
2	0	1/4 CFmax	0	3.91	6.32	6	3.71	7.13	6	3.90	7.09	6
3	0	1/2 CFmax	0	3.83	6.44	6	3.65	7.26	6	3.82	7.24	6
4	0	CFmax	0	3.59	6.87	6	3.44	7.69	6	3.57	7.74	6
5	0	0	1/4 EFmax	3.97	6.21	6	3.77	7.02	6	3.97	6.96	6
6	0	1/4 CFmax	1/4 EFmax	3.90	6.33	6	3.71	7.14	6	3.89	7.10	6
7	0	1/2 CFmax	1/4 EFmax	3.82	6.45	6	3.64	7.27	6	3.81	7.25	6
8	0	CFmax	1/4 EFmax	3.58	6.88	6	3.44	7.69	6	3.57	7.75	6
9	0	0	1/2 EFmax	3.97	6.22	6	3.77	7.03	6	3.96	6.98	6
10	0	1/4 CFmax	1/2 EFmax	3.89	6.34	6	3.70	7.15	6	3.89	7.11	6
11	0	1/2 CFmax	1/2 EFmax	3.82	6.46	6	3.64	7.27	6	3.81	7.26	6
12	0	CFmax	1/2 EFmax	3.58	6.89	6	3.44	7.70	6	3.57	7.75	6
13	0	0	EFmax	3.92	6.30	6	3.73	7.09	6	3.91	7.07	6
14	0	1/4 CFmax	EFmax	3.85	6.41	6	3.67	7.21	6	3.84	7.20	6
15	0	1/2 CFmax	EFmax	3.78	6.53	6	3.61	7.33	6	3.77	7.34	6
16	0	CFmax	EFmax	3.55	6.94	6	3.42	7.75	6	3.54	7.81	6
17	1/4 RLmax	0	0	3.98	6.39	6	3.78	7.21	6	3.98	7.15	6
18	1/4 RLmax	1/4 CFmax	0	3.91	6.51	6	3.71	7.33	6	3.90	7.29	6
19	1/4 RLmax	1/2 CFmax	0	3.83	6.64	6	3.65	7.46	6	3.82	7.44	6
20	1/4 RLmax	CFmax	0	3.59	7.07	6	3.44	7.89	6	3.57	7.94	6
21	1/4 RLmax	0	1/4 EFmax	3.97	6.41	6	3.77	7.22	6	3.97	7.16	6
22	1/4 RLmax	1/4 CFmax	1/4 EFmax	3.90	6.52	6	3.71	7.34	6	3.89	7.30	6
23	1/4 RLmax	1/2 CFmax	1/4 EFmax	3.82	6.65	6	3.64	7.46	6	3.81	7.45	6
24	1/4 RLmax	CFmax	1/4 EFmax	3.58	7.08	6	3.44	7.89	6	3.57	7.94	6
25	1/4 RLmax	0	1/2 EFmax	3.96	6.42	6	3.77	7.23	6	3.96	7.18	6

(*continued on next page*)

Table 8 (*continued*)

Ordinary maintenance every 2 years												
Test	Fault Evolution			New York			Beijing			Vienna		
	RL	CF	EF	SCOP	TEWI [t_{CO2}]	Ninterv.	SCOP	TEWI [t_{CO2}]	Ninterv.	SCOP	TEWI [t_{CO2}]	Ninterv.
26	1/4 RLmax	1/4 CFmax	1/2 EFmax	3.89	6.53	6	3.70	7.34	6	3.89	7.31	6
27	1/4 RLmax	1/2 CFmax	1/2 EFmax	3.82	6.66	6	3.64	7.47	6	3.81	7.46	6
28	1/4 RLmax	CFmax	1/2 EFmax	3.58	7.09	6	3.44	7.90	6	3.57	7.95	6
29	1/4 RLmax	0	EFmax	3.91	6.50	6	3.73	7.29	6	3.91	7.27	6
30	1/4 RLmax	1/4 CFmax	EFmax	3.85	6.61	6	3.67	7.40	6	3.84	7.39	6
31	1/4 RLmax	1/2 CFmax	EFmax	3.78	6.73	6	3.61	7.53	6	3.77	7.53	6
32	1/4 RLmax	CFmax	EFmax	3.55	7.14	6	3.42	7.94	6	3.54	8.01	6
33	1/2 RLmax	0	0	3.97	6.61	6	3.77	7.42	6	3.97	7.36	6
34	1/2 RLmax	1/4 CFmax	0	3.90	6.73	6	3.71	7.54	6	3.89	7.50	6
35	1/2 RLmax	1/2 CFmax	0	3.82	6.85	6	3.64	7.66	6	3.82	7.64	6
36	1/2 RLmax	CFmax	0	3.59	7.27	6	3.44	8.09	6	3.57	8.14	6
37	1/2 RLmax	0	1/4 EFmax	3.96	6.63	6	3.76	7.43	6	3.96	7.38	6
38	1/2 RLmax	1/4 CFmax	1/4 EFmax	3.89	6.74	6	3.70	7.55	6	3.88	7.52	6
39	1/2 RLmax	1/2 CFmax	1/4 EFmax	3.81	6.86	6	3.64	7.67	6	3.81	7.66	6
40	1/2 RLmax	CFmax	1/4 EFmax	3.58	7.28	6	3.44	8.09	6	3.57	8.14	6
41	1/2 RLmax	0	1/2 EFmax	3.94	6.65	6	3.75	7.45	6	3.94	7.41	6
42	1/2 RLmax	1/4 CFmax	1/2 EFmax	3.88	6.76	6	3.69	7.56	6	3.87	7.54	6
43	1/2 RLmax	1/2 CFmax	1/2 EFmax	3.81	6.88	6	3.63	7.68	6	3.80	7.67	6
44	1/2 RLmax	CFmax	1/2 EFmax	3.58	7.29	6	3.44	8.10	6	3.57	8.15	6
45	1/2 RLmax	0	EFmax	3.88	6.76	6	3.70	7.55	6	3.87	7.54	6
46	1/2 RLmax	1/4 CFmax	EFmax	3.82	6.85	6	3.65	7.64	6	3.82	7.64	6
47	1/2 RLmax	1/2 CFmax	EFmax	3.76	6.96	6	3.60	7.75	6	3.75	7.77	6
48	1/2 RLmax	CFmax	EFmax	3.55	7.35	6	3.41	8.15	6	3.53	8.22	6
49	RLmax	0	0	3.83	7.23	6	3.65	8.04	6	3.81	8.04	6
50	RLmax	1/4 CFmax	0	3.78	7.31	6	3.60	8.14	6	3.77	8.13	6
51	RLmax	1/2 CFmax	0	3.73	7.41	6	3.55	8.24	6	3.72	8.23	6
52	RLmax	CFmax	0	3.51	7.82	6	3.38	8.63	6	3.49	8.71	6
53	RLmax	0	1/4 EFmax	3.81	7.27	6	3.63	8.08	6	3.79	8.09	6
54	RLmax	1/4 CFmax	1/4 EFmax	3.76	7.35	6	3.59	8.17	6	3.75	8.17	6
55	RLmax	1/2 CFmax	1/4 EFmax	3.71	7.44	6	3.54	8.27	6	3.70	8.27	6
56	RLmax	CFmax	1/4 EFmax	3.50	7.85	6	3.36	8.66	6	3.48	8.74	6
57	RLmax	0	1/2 EFmax	3.78	7.33	6	3.61	8.13	6	3.76	8.15	6
58	RLmax	1/4 CFmax	1/2 EFmax	3.73	7.40	6	3.56	8.22	6	3.72	8.23	6
59	RLmax	1/2 CFmax	1/2 EFmax	3.69	7.49	6	3.52	8.31	6	3.68	8.32	6

(*continued on next page*)

Table 8 (*continued*)

Ordinary maintenance every 2 years												
Test	Fault Evolution			New York			Beijing			Vienna		
	RL	CF	EF	SCOP	TEWI [t_{CO2}]	Ninterv.	SCOP	TEWI [t_{CO2}]	Ninterv.	SCOP	TEWI [t_{CO2}]	Ninterv.
60	RLmax	CFmax	1/2 EFmax	3.48	7.88	6	3.35	8.69	6	3.46	8.79	6
61	RLmax	0	EFmax	3.68	7.49	6	3.52	8.30	6	3.66	8.35	6
62	RLmax	1/4 CFmax	EFmax	3.65	7.56	6	3.49	8.38	6	3.63	8.41	6
63	RLmax	1/2 CFmax	EFmax	3.61	7.63	6	3.45	8.47	6	3.59	8.48	6
64	RLmax	CFmax	EFmax	3.42	8.00	6	3.30	8.80	6	3.40	8.92	6

Table 9
Values of SCOP, TEWI and number of maintenance interventions depending on the fault intensity evolution and on the climate condition, in case of a 1 year ordinary maintenance strategy

Ordinary maintenance every year												
Test	Fault Evolution			New York			Beijing			Vienna		
	RL	CF	EF	SCOP	TEWI [t_{CO2}]	Ninterv.	SCOP	TEWI [t_{CO2}]	Ninterv.	SCOP	TEWI [t_{CO2}]	Ninterv.
1	0	0	0	3.98	6.19	12	3.78	7.01	12	3.98	6.95	12
2	0	1/4 CFmax	0	3.93	6.27	12	3.74	7.08	12	3.93	7.04	12
3	0	1/2 CFmax	0	3.89	6.35	12	3.69	7.16	12	3.87	7.14	12
4	0	CFmax	0	3.75	6.58	12	3.58	7.40	12	3.72	7.44	12
5	0	0	1/4 EFmax	3.98	6.20	12	3.77	7.02	12	3.97	6.96	12
6	0	1/4 CFmax	1/4 EFmax	3.93	6.28	12	3.73	7.09	12	3.92	7.05	12
7	0	1/2 CFmax	1/4 EFmax	3.88	6.36	12	3.69	7.17	12	3.87	7.15	12
8	0	CFmax	1/4 EFmax	3.74	6.59	12	3.57	7.41	12	3.71	7.44	12
9	0	0	1/2 EFmax	3.97	6.22	12	3.77	7.02	12	3.97	6.97	12
10	0	1/4 CFmax	1/2 EFmax	3.92	6.29	12	3.73	7.10	12	3.91	7.06	12
11	0	1/2 CFmax	1/2 EFmax	3.87	6.37	12	3.69	7.18	12	3.86	7.16	12
12	0	CFmax	1/2 EFmax	3.74	6.60	12	3.57	7.41	12	3.71	7.45	12
13	0	0	EFmax	3.93	6.27	12	3.74	7.07	12	3.93	7.04	12
14	0	1/4 CFmax	EFmax	3.89	6.34	12	3.70	7.15	12	3.88	7.13	12
15	0	1/2 CFmax	EFmax	3.84	6.42	12	3.66	7.22	12	3.83	7.22	12
16	0	CFmax	EFmax	3.71	6.64	12	3.55	7.45	12	3.69	7.50	12
17	1/4 RLmax	0	0	3.98	6.39	12	3.78	7.20	12	3.98	7.15	12
18	1/4 RLmax	1/4 CFmax	0	3.94	6.47	12	3.74	7.28	12	3.93	7.24	12
19	1/4 RLmax	1/2 CFmax	0	3.89	6.55	12	3.69	7.36	12	3.87	7.34	12
20	1/4 RLmax	CFmax	0	3.75	6.78	12	3.58	7.60	12	3.72	7.64	12
21	1/4 RLmax	0	1/4 EFmax	3.98	6.40	12	3.77	7.21	12	3.97	7.16	12
22	1/4 RLmax	1/4 CFmax	1/4 EFmax	3.93	6.48	12	3.73	7.29	12	3.92	7.25	12
23	1/4 RLmax	1/2 CFmax	1/4 EFmax	3.88	6.55	12	3.69	7.37	12	3.87	7.35	12
24	1/4 RLmax	CFmax	1/4 EFmax	3.74	6.79	12	3.57	7.60	12	3.71	7.64	12
25	1/4 RLmax	0	1/2 EFmax	3.97	6.41	12	3.77	7.22	12	3.97	7.17	12

(*continued on next page*)

Table 9 (*continued*)

Ordinary maintenance every year												
Test	Fault Evolution			New York			Beijing			Vienna		
	RL	CF	EF	SCOP	TEWI [t_{CO2}]	Ninterv.	SCOP	TEWI [t_{CO2}]	Ninterv.	SCOP	TEWI [t_{CO2}]	Ninterv.
26	1/4 RLmax	1/4 CFmax	1/2 EFmax	3.92	6.49	12	3.73	7.30	12	3.91	7.26	12
27	1/4 RLmax	1/2 CFmax	1/2 EFmax	3.87	6.56	12	3.69	7.38	12	3.86	7.36	12
28	1/4 RLmax	CFmax	1/2 EFmax	3.74	6.80	12	3.57	7.61	12	3.71	7.65	12
29	1/4 RLmax	0	EFmax	3.93	6.47	12	3.74	7.27	12	3.93	7.24	12
30	1/4 RLmax	1/4 CFmax	EFmax	3.89	6.54	12	3.70	7.34	12	3.88	7.33	12
31	1/4 RLmax	1/2 CFmax	EFmax	3.84	6.62	12	3.66	7.42	12	3.83	7.42	12
32	1/4 RLmax	CFmax	EFmax	3.71	6.84	12	3.55	7.65	12	3.69	7.70	12
33	1/2 RLmax	0	0	3.98	6.59	12	3.78	7.40	12	3.98	7.35	12
34	1/2 RLmax	1/4 CFmax	0	3.93	6.67	12	3.74	7.48	12	3.93	7.44	12
35	1/2 RLmax	1/2 CFmax	0	3.89	6.74	12	3.69	7.56	12	3.87	7.53	12
36	1/2 RLmax	CFmax	0	3.75	6.98	12	3.58	7.80	12	3.72	7.83	12
37	1/2 RLmax	0	1/4 EFmax	3.97	6.60	12	3.77	7.41	12	3.97	7.36	12
38	1/2 RLmax	1/4 CFmax	1/4 EFmax	3.93	6.67	12	3.73	7.49	12	3.92	7.45	12
39	1/2 RLmax	1/2 CFmax	1/4 EFmax	3.88	6.75	12	3.69	7.57	12	3.87	7.54	12
40	1/2 RLmax	CFmax	1/4 EFmax	3.74	6.99	12	3.57	7.80	12	3.71	7.84	12
41	1/2 RLmax	0	1/2 EFmax	3.97	6.61	12	3.77	7.42	12	3.97	7.37	12
42	1/2 RLmax	1/4 CFmax	1/2 EFmax	3.92	6.68	12	3.73	7.49	12	3.92	7.46	12
43	1/2 RLmax	1/2 CFmax	1/2 EFmax	3.87	6.76	12	3.69	7.57	12	3.86	7.56	12
44	1/2 RLmax	CFmax	1/2 EFmax	3.74	6.99	12	3.57	7.81	12	3.71	7.85	12
45	1/2 RLmax	0	EFmax	3.93	6.68	12	3.74	7.47	12	3.92	7.44	12
46	1/2 RLmax	1/4 CFmax	EFmax	3.89	6.74	12	3.71	7.54	12	3.88	7.52	12
47	1/2 RLmax	1/2 CFmax	EFmax	3.84	6.81	12	3.67	7.61	12	3.83	7.61	12
48	1/2 RLmax	CFmax	EFmax	3.71	7.04	12	3.55	7.84	12	3.69	7.90	12
49	RLmax	0	0	3.97	7.01	12	3.77	7.81	12	3.97	7.76	12
50	RLmax	1/4 CFmax	0	3.92	7.08	12	3.73	7.89	12	3.92	7.85	12
51	RLmax	1/2 CFmax	0	3.88	7.15	12	3.69	7.96	12	3.87	7.94	12
52	RLmax	CFmax	0	3.74	7.38	12	3.57	8.20	12	3.72	8.23	12
53	RLmax	0	1/4 EFmax	3.96	7.03	12	3.76	7.83	12	3.96	7.78	12
54	RLmax	1/4 CFmax	1/4 EFmax	3.91	7.09	12	3.72	7.90	12	3.91	7.87	12
55	RLmax	1/2 CFmax	1/4 EFmax	3.87	7.17	12	3.68	7.97	12	3.86	7.95	12
56	RLmax	CFmax	1/4 EFmax	3.74	7.39	12	3.57	8.20	12	3.71	8.24	12
57	RLmax	0	1/2 EFmax	3.94	7.06	12	3.75	7.85	12	3.93	7.82	12
58	RLmax	1/4 CFmax	1/2 EFmax	3.90	7.12	12	3.72	7.91	12	3.90	7.89	12
59	RLmax	1/2 CFmax	1/2 EFmax	3.86	7.18	12	3.68	7.99	12	3.85	7.97	12

(*continued on next page*)

Table 9 (*continued*)

Ordinary maintenance every year												
Test	Fault Evolution			New York			Beijing			Vienna		
	RL	CF	EF	SCOP	TEWI [t_{CO2}]	Ninterv.	SCOP	TEWI [t_{CO2}]	Ninterv.	SCOP	TEWI [t_{CO2}]	Ninterv.
60	RLmax	CFmax	1/2 EFmax	3.73	7.40	12	3.57	8.21	12	3.71	8.25	12
61	RLmax	0	EFmax	3.88	7.15	12	3.70	7.95	12	3.87	7.94	12
62	RLmax	1/4 CFmax	EFmax	3.85	7.20	12	3.67	8.00	12	3.84	8.00	12
63	RLmax	1/2 CFmax	EFmax	3.82	7.25	12	3.64	8.06	12	3.80	8.06	12
64	RLmax	CFmax	EFmax	3.71	7.45	12	3.55	8.25	12	3.68	8.31	12

References

[1] F. Pelella, L. Viscito, A.W. Mauro, Combined effects of refrigerant leakages and fouling on air-source heat pump performances in cooling mode, Appl. Therm. Eng. 204 (2022) 117965.
[2] IEA (International Energy Agency), Energy Statistics Data Browser, 2022. Paris, https://www.iea.org/data-and-statistics/data-tools/energy-statistics-data-browser.
[3] M. Maasoumy, A. Sangiovanni-Vincentelli, Smart connected buildings design automation: Foundations and trends in Electronic Design Automation, 1–2 10, 2016, pp. 1–143.
[4] COP26 Presidency Outcomes, The Glasgow Climate Pact, November 2021. *Glasgow*, https://ukcop26.org/wp-content/uploads/2021/11/COP26-Presidency-Outcomes-The-Climate-Pact.pdf.
[5] V. Masson-Delmotte, P. Zhai, H.O. Pörtner, D. Roberts, J. Skea, P.R. Shukla, T. Waterfield, Global Warming of 1.5 C. An IPCC Special Report on the Impacts of Global Warming of, 1.5, 2018.
[6] R. Mastrullo, A.W. Mauro, G. Napoli, F. Pelella, L. Viscito, Flow boiling of azeotropic and nonazeotropic mixtures. Effect of the glide temperature difference on the nucleate boiling contribution: assessment of methods, in: Journal of Physics: Conference Series, vol. 1599, IOP Publishing, 2020, 012053. No. 1.
[7] A.W. Mauro, G. Napoli, F. Pelella, L. Viscito, Flow boiling heat transfer and pressure drop data of non-azeotropic mixture R455A in a horizontal 6.0 mm stainless-steel tube, Int. J. Refrig. 119 (2020) 195–205.
[8] G. Lillo, R. Mastrullo, A.W. Mauro, F. Pelella, L. Viscito, Experimental thermal and hydraulic characterization of R448A and comparison with R404A during flow boiling, Appl. Therm. Eng. 161 (2019), 114146.
[9] A.W. Mauro, G. Napoli, F. Pelella, L. Viscito, Flow pattern, condensation and boiling inside and outside smooth and enhanced surfaces of propane (R290). State of the art review, Int. J. Heat Mass Tran. 174 (2021), 121316.
[10] C. Francis, G. Maidment, G. Davies, An investigation of refrigerant leakage in commercial refrigeration, Int. J. Refrig. 74 (2017) 12–21.
[11] T.M. Rossi, J.E. Braun, A statistical, rule-based fault detection and diagnostic method for vapor compression air conditioners, HVAC R Res. 3 (1997) 19–37.
[12] B. Citarella, A.W. Mauro, F. Pelella, in: Use of Artificial Intelligence in the Refrigeration Field, 6th IIR TPTPR Conference, vols. 1–3, Vicenza, Italy, 2021, https://doi.org/10.18462/iir.TPTPR.2021.2061. September.
[13] M.S. Mirnaghi, F. Haghighat, Fault detection and diagnosis of large-scale HVAC systems in buildings using data-driven methods: a comprehensive review, Energy Build. 229 (2020).
[14] A. Afram, F. Janabi-Sharifi, Review of modeling methods for HVAC systems, Appl. Therm. Eng. 67 (2014) 507–519.
[15] A. Afram, F. Janabi-Sharifi, A.S. Fung, K. Raahemifar, Artificial neural network (ANN) based model predictive control (MPC) and optimization of HVAC systems: a state of the art review and casestudy of a residential HVAC system, Energy Build. 141 (2017) 96–113.
[16] M.C. Comstock, J.E. Braun, Development of Analysis Tools for the Evaluation of Fault Detection and Diagnostics in Chillers ASHRAE Research Project 1043-RP; Also Ray W. Herrick Laboratories, Purdue University, 1999.
[17] M.S. Breuker, J.E. Braun, Common Fault and their impacts for rooftop air conditioners, HVAC R Res. 4 (1998) 303–318.
[18] J. Kim, S. Frank, J.E. Braun, D. Goldwasser, Representing small commercial building faults in EnergyPlus, Part I: model development, Buildings 9 (2019) 233.
[19] I.N. Grace, D. Datta, S.A. Tassou, Sensitivity of refrigeration system performance to charge levels and parameters for on-line leak detection, Appl. Therm. Eng. 25 (2005) 557–566.
[20] I. Bellanco, F. Belío, M. Vallés, R. Gerber, J. Salom, Common fault effects on a natural refrigerant, variable-speed heat pump, Int. J. Refrig. 133 (2022) 259–266.
[21] B.A. Qureshi, S.M. Zubair, The impact of fouling on the condenser of a vapor compression refrigeration system: an experimental observation, Int. J. Refrig. 38 (2014) 260–266.
[22] M. Mehrabi, D. Yuill, Fouling and its effects on air-cooled condensers in split system air conditioners (RP-1705), Sci. Technol. Built Environ. 25 (2019) 784–793.
[23] Y. Hu, D.P. Yuill, A. Ebrahimifakhar, A. Rooholghodos, An experimental study of the behavior of a high efficiency residential heat pump in cooling mode with common installation faults imposed, Appl. Therm. Eng. 184 (2021) 116116.
[24] M. Mehrabi, D. Yuill, Generalized effects of refrigerant charge on normalized performance variables of air conditioners and heat pumps, Int. J. Refrig. 76 (2017) 367–384.
[25] M. Mehrabi, D. Yuill, Generalized effects of faults on normalized performance variables of air conditioners and heat pumps, Int. J. Refrig. 85 (2018) 409–430.
[26] Y. Hu, D.P. Yuill, Effects of multiple simultaneous faults on characteristic fault detection features of a heat pump in cooling mode, Energy Build. 251 (2021), 111355.
[27] Z. Zhou, H. Chen, L. Xing, G. Li, W. Gou, An experimental study of the behavior of a model variable refrigerant flow system with common faults, Appl. Therm. Eng. 202 (2022) 117852.
[28] R. Mastrullo, A.W. Mauro, F. Pelella, L. Viscito, Dual source (air-solar) heat pump: thermo-economic analysis of sizing factors depending on climate conditions, 15th IIR-Gustav Lorentzen Conference on Natural Refrigerants, June 13-15, Trondheim, Norway.
[29] A.W. Mauro, G. Napoli, F. Pelella, L. Viscito, Numerical Analysis of a Solar-Assisted Dual-Source Heat Pump Coupled with a Thermal Storage for Residential Heating, 16th International Conference of Heat Transfer, Fluid Mechanics and Thermodynamics (HEFAT), Virtual, 8-10 August 2022.
[30] F. Pelella, G. Zsembinszki, L. Viscito, A.W. Mauro, L.F. Cabeza, Thermo-economic optimization of a multi-source (air/sun/ground) residential heat pump with a water/PCM thermal storage, Appl. Energy 331 (2023), 120398.
[31] R.K. Shah, D.P. Sekulic, Fundamental of Heat Exchanger Design, John Wiley & Sons, 2003.
[32] K. Gungor, R. Winterton, A general correlation for flow boiling in tubes and annuli, Int. J. Heat Mass Tran. 29 (1986) 351–358.
[33] M.M. Shah, A general correlation for heat transfer during film condensation inside pipes, Int. J. Heat Mass Tran. 22 (1979) 547–556.
[34] F.W. Dittus, L.M.K. Boelter, Heat transfer in automobile radiators of the tubular type, Univ. Calif. Publ. Entomol. 2 (1930) 443–461.

[35] C.C. Wang, Y.Y. Chi, Heat transfer and friction characteristics of plain fin-and-tube heat exchangers: Part II. Correlation, Int. J. Heat Mass Tran. 43 (2000) 2693–2700.
[36] T.E. Schmidt, Heat transfer calculations for extended surfaces. Refrigerating Engineering 57 (1949) 351–357.
[37] Z. Rouhani, E. Axelsson, Calculation of volume void fraction in a subcooled and quality region, Int. J. Heat Mass Tran. 17 (1970) 383–393.
[38] F. Pelella, L. Viscito, A.W. Mauro, Soft faults in residential heat pumps: possibility of evaluation via on-field measurements and related degradation of performance, Energy Convers. Manag. 260 (2022), 115646.
[39] L. Yang, J.E. Braun, E.A. Groll, The Role of Filtration in Maintaining Clean Heat Exchanger Coils, Air-Conditioning and Refrigeration Technology Institute, 2004.
[40] A.H.H. Ali, I.M. Ismail, Evaporator air-side fouling: effect on performance of room air conditioners and impact on indoor air quality, HVAC R Res. 14 (2008) 209–219.
[41] B.C. Pak, E.A. Groll, J.E. Braun, Impact of Fouling and Cleaning on Plate Fin and Spine Fin Heat Exchanger Performance, vol. 111, Ashrae Transaction, 2005.
[42] J.A. Siegel, W.W. Nazaroff, Predicting particle deposition on HVAC heat exchangers, Atmos. Environ. 37 (2003) 5587–5596.
[43] Commission Regulation (EU), *Implementing Directive 2009/125/EC of the European Parliament and of the Council Establishing a Framework for the Setting of Ecodesign Requirements for Energy-Related Products,* with Regard to Ecodesign Requirements for Air Heating Products, Cooling Products, High Temperature Process Chillers and Fan Coil Units (Text with EEA Relevance), 2016/2281 of 30 November 2016.
[44] IIR (International Institute of Refrigeration), 24th Informative Note on Refrigeration Technologies, January 2014.
[45] M. Awais, A.A. Bhuiyan, Recent advancements in impedance of fouling resistance and particulate depositions in heat exchangers, Int. J. Heat Mass Tran. 141 (2019) 580–603.
[46] M.C. Comstock, J.E. Braun, E.A. Groll, The sensitivity of chiller performance to common faults, HVAC R Res. 7 (2001) 263–279.